



UNIVERSIDADE D
COIMBRA

Nuno Miguel Rebelo Brito

**LATTICE COMPUTATION OF THE KUGO-OJIMA
CORRELATION FUNCTION**

**Dissertação no âmbito do Mestrado em Física orientada pelo Professor
Doutor Orlando Olavo Aragão Aleixo e Neves de Oliveira e Doutor Paulo de
Jesus Henriques da Silva e apresentada ao Departamento da Física da
Faculdade de Ciências e Tecnologia da Universidade de Coimbra.**

Setembro de 2023



UNIVERSIDADE D
COIMBRA

Lattice Computation of the Kugo-Ojima Correlation Function

Supervisors:

Prof Dr. Orlando Olavo Aragão Aleixo e Neves de Oliveira
Dr. Paulo de Jesus Henriques da Silva

Jury:

Prof. Dr. Pedro Almeida Vieira Alberto
Dr. Paulo de Jesus Henriques da Silva
Prof. Dr. David Henk Dudal

Dissertation submitted in partial fulfillment for the degree of Master of Science in
Physics.

Coimbra, September, 2023

Acknowledgments

I would like to start by expressing my deepest gratitude towards my advisors Prof. Dr. Orlando Oliveira and Dr. Paulo Silva, for their patience and guidance throughout the past year, as well as very valuable advice. I have learned so much about a lot of things, ranging from Physics to the world of Physics research and for that I am very thankful. It is far from easy to work with someone completely new whose work dynamics are unknown and I am aware that especially in my case, it might have been challenging. Their contributions towards this dissertation were incredibly vital and I dearly appreciate their endless patience.

I am also very grateful for the collaboration and fruitful discussions with Dr Joannis Papavassiliou and Dr. Mauricio Ferreira from the University of Valencia.

To my friends group *SU(5)* who stuck together throughout the insanity that was the first years of the Master's Degree, thank you for putting up with me in our darkest hours.

To my friends group *Phelps* and *Dia D*, thank you for the good company during this and the last year. It gets quite lonely being a graduate student, we often grow apart from our previous acquaintances.

To my closest friend group, thank you, for the good and bad times, for the fun and the boring, for the hype and for the down times. We built an awesome story together and I can only wish that I could have been more present. Special thanks to Benitake, Ramon, Bruno the Giant, Cravo and Afonso and Carrasco.

To my colleague Helena, who has been the literal impersonation of "Same" throughout this year. Whether the ship was afloat or sinking we were on it.

To Tânia who has probably been the first person I met who has shown me her unfiltered appreciation for me, something that I had not known how it felt for a long time. Although we might grow apart, you surely left a good mark on me.

To all my acquaintances in Coimbra, thank you. I did not hesitate in choosing the Physics

Department in Coimbra and I'm glad for that. It was an awesome place to study and to be a student if you know what I mean.

Thank you Hakita for designing and making the awesome game that is *ULTRAKILL* which has entertained me so much throughout these last two years.

Now, onto the two most important acknowledgements. To my family, who have been undeniably and unconditionally a huge support pillar for me. Thank you Mother for being, objectively might I add, the best mother in the world. Thank you Father for the calm and wise advice, which has helped me become a version of myself that I am very proud of. Thank you Brother for being my life advisor and for the valuable life advice.

And finally, to my girlfriend Cláudia, who has undoubtedly changed my life for the good, for the endless support, love and company. This year was very hard, and that difficulty would only increase exponentially if it were not for you. You are most certainly the best thing that has happened to me during my time in Coimbra.

This work was supported with funds from the Portuguese National Budget through Fundação para a Ciência e Tecnologia (FCT) under the projects UIDB/04564/2020 and UIDP/04564/2020. The author acknowledges the Laboratory for Advanced Computing at the University of Coimbra (<http://www.uc.pt/lca>) for providing access to the HPC resources that have contributed to the research within this paper. Access to Navigator was partly supported by the FCT Advanced Computing Projects 2021.09759.CPCA and 2022.15892.CPCA.A2. The author also acknowledges the computing resources provided by the Partnership for Advanced Computing in Europe (PRACE) initiative under DECI-9 project COIMBRALATT and DECI-12 project COIMBRALATT2.

Torro(z/s)elo, Setembro de 2023

Resumo

Atualmente, o confinamento da cor na Cromodinâmica Quântica permanece um mistério do ponto de vista teórico. Até hoje, não foi encontrada prova analítica para o confinamento de cor, e o mecanismo responsável pelo confinamento dos estados com cor do subespaço de estados físicos é ainda desconhecido. Taichiro Kugo e Izumi Ojima propuseram um mecanismo de confinamento baseado na simetria BRST e derivaram assim os requerimentos para o realização deste mecanismo. Um desses requerimentos, que por sua vez é o menos óbvio, é que uma função de correlação especial, chamada *Função de correlação de Kugo-Ojima* $u(p^2)$ tende para -1 na origem ($p^2 = 0$). Esta função pode ser obtida na rede usando a formulação de teorias de gauge na rede.

Este trabalho consiste nos resultados da rede para esta função de correlação na gauge de Landau. Apresentam-se os resultados para 4 redes simétricas de grande volume ($32^4, 48^4, 64^4, 80^4$) com $\beta = 6.0$ na gauge de Landau. Testes relativamente à transversalidade da função de Kugo-Ojima também são feitos assim como também considerações estatísticas dos resultados. Os resultados apresentam mais provas que o mecanismo de confinamento de Kugo-Ojima não é realizado e que a função de correlação de Kugo-Ojima, na gauge the Landau, é de facto transversa. Os nossos resultados alinham-se qualitativamente com literatura existente, contribuindo para o nosso entendimento de Cromodinâmica Quântica. Esta esforço atual para descrever o fenómeno de confinamento de cor permanece com um desafio central em Física de Partículas.

Palavras-Chave: Confinamento de cor, QCD na rede, Função de Kugo-Ojima, Teoria Quântica de Campos, Gauge de Landau.

Abstract

As of today, color confinement in Quantum Chromodynamics remains a mystery from the theoretical point of view. So far, no analytical proof of color confinement has been found and the mechanism that confines colored states from the space of physical states is still unknown. Taichiro Kugo and Izumi Ojima proposed such confinement mechanism, using as basis the BRST-symmetry and derived the requirements for the realization of this mechanism. One such requirement, which happens to be the non-trivial one, is that a special correlation function, the *Kugo-Ojima correlation function* $u(p^2)$, approaches -1 at the origin ($p^2 = 0$). This correlation function can be obtained on the lattice within the lattice formulation of gauge theories.

The present work consists on lattice results for this correlation function on the Landau gauge. We present results obtained from 4 symmetric large volume lattices ($32^4, 48^4, 64^4, 80^4$) with $\beta = 6.0$ on the Landau gauge. A test on the transversality of the Kugo-Ojima correlation function is also performed, along with some statistical considerations of the results. The results present further evidence that the Kugo-Ojima confinement scenario is not realized on the lattice and that the Kugo-Ojima correlation function, in the Landau gauge, is transverse. Our findings align qualitatively with existing literature, contributing to our understanding of Quantum Chromodynamics. This ongoing pursuit to unravel color confinement remains a central challenge in particle physics.

Keywords: Color Confinement, Lattice QCD, Kugo-Ojima function, Quantum Field Theory, Landau Gauge.

Luck is what happens when preparation meets opportunity.

Lucilius Seneca

Contents

Acknowledgements	ii
Resumo	iv
Abstract	v
List of Figures	xi
List of Tables	xii
1 Introduction	2
2 Basics of Quantum Chromodynamics	5
2.1 QCD Lagrangian	5
2.2 Path Integral Formulation	7
2.2.1 Euclidean Field Theory	8
2.2.2 Faddeev-Popov Procedure	8
2.2.3 The Gribov Copies Problem	9
2.3 Regularization and Renormalization	10
2.3.1 Regularization	10
2.3.2 Renormalization	11
3 Kugo Ojima Confinement Scenario	13
3.1 Preliminary Properties	13
3.2 Defining the Hilbert Space	16
3.2.1 Physical Subspace and BRST-Algebra	17
3.2.2 Inner Product Structure	17
3.2.3 The Quartet Mechanism	18

3.3	Color Confinement	20
4	Lattice Computation of the Kugo-Ojima function	23
4.1	Lattice Discretization	23
4.2	Gauge Fields on the Lattice	24
4.3	Numerical Aspects	26
4.3.1	Lattice Observables	26
4.3.2	Gauge Fixing	27
4.4	The Lattice Kugo-Ojima function	28
4.4.1	Computational Recipe	29
4.4.2	Longitudinal Test	32
4.4.3	Lattice Artifacts	33
5	Results and Discussion	34
5.1	The Bare Kugo-Ojima function	35
5.2	Longitudinal Test	38
5.3	Inclusion of Negative Momenta Points	40
5.4	Sources vs Configurations	41
5.5	H4 method	42
5.6	Renormalization of the Kugo-Ojima function	43
6	Conclusion	46
	Bibliography	47
A	Parallel Transporter	53
B	Gauge Fixing Functional	55
C	Point Source Generation	56

List of Figures

4.1	The Plaquette as a closed loop of links. The definition in (4.10) was used. Image from [1].	25
5.1	The function $u(p^2)$ for all lattice volumes.	35
5.2	All the previous plots combined.	36
5.3	Infrared behaviour of the Kugo-Ojima function.	36
5.4	Longitudinal component $L(q)$ of the lattice Kugo-Ojima function.	38
5.5	Effect of including negative momenta in Z_4 averaging process for the 80^4 lattice. All plots have been computed over a single source.	40
5.6	Difference between using sources vs configurations.	41
5.7	Comparing the H4 method with the cuts discussed in 4.4.3 for the Kugo- Ojima function $u(p^2)$ and its dressing function $K(p^2)$. Both plots have been computed with 200 configurations over 1 source.	42
5.8	The renormalized lattice Kugo-Ojima function compared with the results of [2]. The vertical black bar denotes the $q = 4.3$ GeV line.	43
5.9	Previous figure but in logarithmic scale.	44

List of Tables

5.1	Configuration setup of this work.	34
-----	---	----

1 Introduction

Particle Physics is the area of physics concerned with describing the dynamics of matter at the atomic and sub-atomic level. One of its most successful theories is the Standard Model, which provides a description for three of the four fundamental interactions in nature: strong, weak and electromagnetic interaction. The fourth fundamental interaction, gravity, still lacks a quantum description.

The Standard Model is a gauge theory based on the gauge group $SU(3) \otimes SU(2) \otimes U(1)$ and it provides an unified description of the dynamics and symmetries of fundamental particles. A fundamental symmetry of the Standard Model Lagrangian is the gauge symmetry that is associated with the gauge group. Indeed, the equations of motion derived from the Lagrangian are invariant under gauge transformations.

The Standard Model Lagrangian is divided into sectors, each of which is responsible for the description of different fundamental particles and their interactions. The electromagnetic and the weak interaction are unified into the electroweak sector, with gauge group $SU(2) \otimes U(1)$. The strong sector, associated with the gauge group $SU(3)$, describes the interactions between quarks and gluons. The theory of the strong interaction is called Quantum Chromodynamics (QCD).

Quantum Electrodynamics (QED) is the theory of the electromagnetic interaction and it defines the interactions of charged particles such as electrons and photons. The perturbative description of QED has provided highly satisfactory experimental predictions, but the same case cannot be said for QCD. Many features of QCD can only be described in a non-perturbative scheme, one such feature is color confinement. Color is a property inherent to the elemental particles of QCD that can be thought of as the analogue of the electric charge of QED. Color confinement consists of how the fundamental quanta of QCD are not observed asymptotically unlike the photon or the electron. More specifically, colored particles are not observed experimentally as free particles.

This leads to the hypothesis that colored states do not belong to the physical Hilbert space of QCD, similar to how longitudinally polarized photons are excluded from the physical subspace in the Gupta-Bleuler quantization of QED [3, 4]. However, as of today, a theoretical proof of color confinement does not exist but there have been proposals for a color confinement mechanism. One such proposition was provided in 1979 by Taichiro Kugo and Izumi Ojima [5].

Their work extended well beyond addressing color confinement; they provided a thorough and detailed description of the Canonical Quantization of Yang-Mills theories. The color confinement mechanism proposed by them used the BRST-symmetry [6, 7], a generalized type of gauge symmetry, to define the Hilbert space of physical states. Then, they prove that every state in this space is a color singlet, but only if two requirements are satisfied. One of these requirements is that the color symmetry remains unbroken, which they assume given the observed phenomenon of color confinement. The other is that a certain correlation function, called the *Kugo-Ojima correlation function* $u(p^2)$ converges to -1 at the origin. Kugo also showed that if this requirement is satisfied, the ghost dressing function would also diverge [8] at the origin.

The interest in this function spans beyond color confinement. The function is conceptually connected within the Gribov-Zwanziger framework [9, 10, 11] and it is a necessary ingredient for other formulations of Yang-Mills theories (see [2] or Chapter 2 of [12] and references therein).

To study this function, non-perturbative methods must be used, such as the Lattice formulation of Gauge theories and the Dyson-Schwinger equations. The Lattice formulation discretizes space-time, providing a very convenient framework to simulate Gauge theories on a computer and will be the one we will use. The computation of this function, as well as its properties, is the focus of this work. We intend to provide, using the Lattice formulation of gauge theories, a numerical computation of the Kugo-Ojima correlation function using a large lattice volume.

This work is organized as follows: In the next chapter, we give a brief introduction of Quantum Chromodynamics. In the third chapter, the background of the Kugo-Ojima correlation function is explained and the Kugo-Ojima confinement scenario's necessary ingredients are stated. In the fourth chapter, we present the lattice formulation of Gauge Theories and use this formulation to compute the Kugo-Ojima function on the Lattice.

Finally, we give a short insight into the obtained results as well as plans for the future.

2 Basics of Quantum Chromodynamics

In this chapter, the basic definitions of QCD are given, namely the Lagrangian and its symmetries. The path-integral formulation of field theories is also discussed, as well as how to extract the Green's functions of the theory. The procedures of renormalization and regularization are briefly discussed.

2.1 QCD Lagrangian

Quantum Chromodynamics is formulated under the Lagrangian framework. This framework allows the description of the dynamics of the theory as well as the underlying symmetries. At its core is the Lagrangian density:

$$\mathcal{L}_{QCD} = \sum_f \bar{\psi}_f (i\gamma^\mu \nabla_\mu - m_f) \psi_f - \frac{1}{4} F_{\mu\nu}^a F^{a\mu\nu}. \quad (2.1)$$

Here, ψ_f denotes the flavored f-quark spinor field, $\bar{\psi}_f = \psi_f^\dagger \gamma^0$. We use latin indices to denote the color component of the fields, and greek ones to denote the Lorentz component. Additionally, if any indices (greek or latin) are repeated, a sum over its values is to be intended. The covariant derivative ∇_μ is given by:

$$\nabla_\mu \psi \equiv \nabla_\mu^{ab} \psi^b = (\delta^{ab} \partial_\mu + ig [t^c]^{ab} A_\mu^c) \psi^b. \quad (2.2)$$

The real-valued fields A_μ^c are the components of the linear combination of the gauge field $A_\mu(x) \equiv A_\mu^c(x) t^c$. This gauge field is an element of the SU(3) Lie Algebra, and its introduction is necessary to maintain the gauge invariance of the theory. The t^c are the 8 generators of a given representation of Lie Algebra of SU(3) ($c = 1, \dots, 8$). This algebra is characterized by the following relations:

$$[t^a, t^b] = if^{abc} t^c, \quad \text{Tr}(t^a t^b) = R \delta^{ab}. \quad (2.3)$$

In this work, the fundamental and the adjoint representations will be considered. The value of R also depends of the representation (for $SU(N)$, $R = \frac{1}{2}$ for the fundamental representation, $R = N$ for the adjoint representation). So, we set the following notation for the covariant derivative in these two representations:

$$\begin{aligned} [\nabla_\mu(x)]^{ab} &\equiv \left(\delta^{ab} \frac{\partial}{\partial x^\mu} + ig \frac{[\lambda^c]^{ab}}{2} A_\mu^c(x) \right), \\ [D_\mu(x)]^{ab} &\equiv \left(\delta^{ab} \frac{\partial}{\partial x^\mu} + g f^{abc} A_\mu^c(x) \right). \end{aligned} \quad (2.4)$$

We reserve the notation t^a for the fundamental representation while for the adjoint representation we substitute explicitly $[t^a]^{bc} = -if^{abc}$. In the case of the Lagrangian density (2.1), the covariant derivative of the spinor quark field is in the fundamental representation. The Field Strength tensor $F_{\mu\nu}^a$ is given by:

$$F_{\mu\nu}^a = \partial_\mu A_\nu^a - \partial_\nu A_\mu^a + g(A_\mu \times A_\nu)^a \quad \text{where} \quad (A_\mu \times A_\nu)^a \equiv f^{abc} A_\mu^b A_\nu^c. \quad (2.5)$$

Equipped with the Lagrangian Density, the action is written as:

$$S[\psi, \bar{\psi}, A_\mu] = \int d^4x \mathcal{L}[\psi, \bar{\psi}, A_\mu] \quad (2.6)$$

and we obtain the respective equations of motion for the fields setting the first variation of the action to zero $\delta S = 0$:

$$\begin{aligned} (D_\nu F^{\mu\nu})^a &= \bar{\psi} \gamma^\mu t^a \psi, \\ (i\gamma^\mu \nabla_\mu + m)^{ab} \psi^b &= 0, \\ \bar{\psi}^a (i\gamma^\mu \nabla_\mu + m)^{ab} &= 0. \end{aligned} \quad (2.7)$$

The Lagrangian density also reflects the underlying symmetries of the theory. QCD is a $SU(3)$ Non-Abelian gauge theory, meaning that (2.1) is invariant under local $SU(3)$ transformations:

$$\begin{aligned} \psi(x) &\longrightarrow \psi^G(x) = G(x)\psi(x), \\ \bar{\psi}(x) &\longrightarrow \bar{\psi}^G(x) = \bar{\psi}(x)G^\dagger(x), \\ A_\mu(x) &\longrightarrow A_\mu^G(x) = G(x)A_\mu(x)G^\dagger(x) - \frac{i}{g}G(x)\partial_\mu G^\dagger(x). \end{aligned}$$

Where $G(x) = e^{ig\alpha^a(x)t^a}$ is a element of the $SU(3)$ Lie Group, so that $G^{-1}(x) = G^\dagger(x)$. It is often simpler to workout the derivation for a infinitesimal gauge transformation since we can build the finite transformation by sucessively applying infinitesimal transformations.

The infinitesimal version of the transformation laws in (2.8) become:

$$G(x) \approx (\mathbf{1} + ig\alpha^a(x)t^a + \mathcal{O}(g^2)) \implies \begin{cases} \psi^G(x) = (\mathbf{1} + ig\alpha^a(x)t^a + \mathcal{O}(g^2))\psi(x), \\ \bar{\psi}^G(x) = \bar{\psi}(x)(\mathbf{1} - ig\alpha^a(x)t^a + \mathcal{O}(g^2)), \\ (A^G)_\mu^a(x) = A_\mu^a(x) + \frac{1}{g}\partial_\mu\alpha^a(x) + f^{abc}A_\mu^b(x)\alpha^c(x). \end{cases} \quad (2.8)$$

The components $(A^G)_\mu^a(x)$ are calculated by projecting A_μ onto the generators t^a using the trace property in (2.3) in the following way:

$$(A^G)_\mu^a(x) = \frac{1}{R} \text{Tr}\{A_\mu^G(x)t^a\}. \quad (2.9)$$

2.2 Path Integral Formulation

The Path Integral formulation of quantum mechanics was originally created by Feynman [13]. This formulation allows the generalization of the principle of least action from classical mechanics into quantum mechanics, in a way such that every possible trajectory contributes (or interferes) to the probability amplitude of a given process. In the path integral formulation of quantum field theory, the central object is the *generating functional* [14], which is the vacuum-vacuum amplitude:

$$\langle 0 | 0 \rangle_J = Z[J_1, \dots, J_n] = \int \mathcal{D}\phi_1 \dots \mathcal{D}\phi_n e^{iS[\phi_1, \dots, \phi_n] + i \int d^4x \sum_i \phi_i(x) J_i(x)} \quad (2.10)$$

where J_i is the source of the field ϕ_i . The *Green's functions* (or correlation functions) of the theory can be derived through consecutive functional derivation of (2.10):

$$\begin{aligned} \langle 0 | T(\phi_1(x_1) \dots \phi_n(x_n)) | 0 \rangle &= \left. \frac{\delta^n Z[J_1, \dots, J_n]}{\delta J_1(x_1) \dots \delta J_n(x_n)} \right|_{J=0} \equiv G^{(n)}(x_1, \dots, x_n) \\ &= \frac{1}{Z[0, \dots, 0]} \int \mathcal{D}\phi_1 \dots \mathcal{D}\phi_n (\phi_1(x_1) \dots \phi_n(x_n)) e^{iS[\phi_1, \dots, \phi_n]} \end{aligned}$$

where T is the time-ordering operator. These functions are objects of interest since their knowledge allows us to extract relevant properties and quantities of the system [15]. As an example, Feynman diagrams are built using these functions and allow writing diagrammatically probability amplitudes of relevant processes of the theory. It is also possible to define the Green's functions in momentum space:

$$\begin{aligned} G^{(n)}(p_1, \dots, p_n) (2\pi)^4 \delta(p_1 + \dots + p_n) &= \\ = \int d^4x_1 \dots d^4x_n e^{-i(p_1x_1 + \dots + p_nx_n)} G^{(n)}(x_1, \dots, x_n). \end{aligned} \quad (2.11)$$

The momentum space Green's functions are often preferred instead of (2.11), since their expressions are often simpler than their coordinate-space counterpart. As a result, the expressions for Feynman diagrams are further simplified [15]. The delta function included on the left-hand side accounts for momentum conservation.

2.2.1 Euclidean Field Theory

Quantities such as (2.10) can't be evaluated exactly most of the times. The integrand contains an exponential with an oscillatory phase which rises convergence problems in (2.10)¹. Consequently, it is often performed a *Wick's rotation*, which consists of an analytical continuation into the complex plane, by setting:

$$t = e^{-i\frac{\pi}{2}} t_E = -it_E \quad (2.12)$$

which implies that the generating functional (2.10) is now written as:

$$Z[J_1, \dots, J_n] = \int \mathcal{D}\phi_1 \dots \mathcal{D}\phi_n e^{-S[\phi_1, \dots, \phi_n] + \int d^4x \sum_i \phi_i(x) J_i(x)}. \quad (2.13)$$

If the Euclidean version of the theory satisfies the Osterwalder-Schrader's axioms [16], then the corresponding Green's functions of the theory may be analytically continued back into the Minkowskian space-time theory. So, one can work with the theory in its Euclidean version (2.13), and then return to the Minkowski space-time. However, the analytical continuation back to the Minkowski space-time might not be valid in the non-perturbative regime, but if we work with the Euclidean version of the theory, we need not to return to the Minkowski space-time.

2.2.2 Faddeev-Popov Procedure

As a consequence of the gauge invariance, the action is also gauge invariant:

$$S[A_\mu^G, \psi^G, \bar{\psi}^G] = S[A_\mu, \psi, \bar{\psi}] \quad (2.14)$$

where A_μ^G is the transformed gauge field as in (2.8). For simplicity, let's consider only the gauge part of the generating functional:

$$Z_G[\omega^\mu] = \int \Pi_\mu \mathcal{D}A_\mu e^{-S[A_\mu] - \int d^4x \omega^\mu(x) A_\mu(x)}. \quad (2.15)$$

¹There are some exceptions to this, such as Free Field theories where we can use some the functional version of some gaussian identities.

The problem with formula (2.15) is that for a given A_μ there are an infinite number of gauge-related gauge fields, which spoils the functional integration $\Pi_\mu \mathcal{D}A_\mu$. To proceed, one has to restrict the integration so that we have a single representative per gauge orbit². Faddeev and Popov [17] have shown how to achieve such by imposing a condition on the space of the gauge fields A_μ of the type:

$$F[A; x] = 0. \quad (2.16)$$

In this work, the Landau Gauge is considered, which means imposing:

$$F[A; x] = \partial^\mu A_\mu(x) \implies F[A; x]^a \equiv \partial^\mu A_\mu^a(x) = 0. \quad (2.17)$$

The details regarding this procedure may be found in the original paper by Faddeev and Popov [17] or in any standard textbook [14, 18, 19]. The resulting generating functional after the Faddeev-Popov procedure is written as:

$$Z[\eta, \bar{\eta}, \omega^\mu, \sigma, \bar{\sigma}] = \int \mathcal{D}A_\mu \mathcal{D}\psi \mathcal{D}\bar{\psi} \mathcal{D}c \mathcal{D}\bar{c} \exp\{iS[\psi, \bar{\psi}, A_\mu]\} \exp\left\{i \int d^4x \left(\mathcal{L}_{FP} + \mathcal{L}_{GF} + \omega^{a\mu} A_\mu^a + \bar{\eta}^a \psi^a + \bar{\psi}^a \eta^a + \bar{c}^a \sigma^a + \bar{\sigma}^a c^a\right)\right\} \quad (2.18)$$

where:

$$\begin{aligned} \mathcal{L}_{FP} &= \bar{c}^a \partial^\mu (D_\mu c)^a, \\ \mathcal{L}_{GF} &= -\frac{1}{2\xi} (\partial^\mu A_\mu^a)^2. \end{aligned} \quad (2.19)$$

The fields c and \bar{c} are called *ghost fields* and they are Grassmann variables. The inclusion of these fields allows writing the restriction that (2.16) imposes on the integration $\Pi_\mu \mathcal{D}A_\mu$ as a simple exponential factor in the generating functional (2.18) [19]. The *effective Lagrangian Density* is defined as:

$$\mathcal{L}_{\text{eff}} = \mathcal{L}_{QCD} + \mathcal{L}_{FP} + \mathcal{L}_{GF}. \quad (2.20)$$

2.2.3 The Gribov Copies Problem

However, it has been proven that for the case of non-perturbative QCD, as well as with other Non-Abelian Gauge Theories, that the Faddeev-Popov procedure fails. Namely, (2.17) is not able to select a single representative per orbit, which is also known as the Gribov Copies Problem [20]. Furthermore, it has been proven that for a four-dimensional

²A gauge orbit is the set of gauge fields related by a gauge transformation.

sphere [21] and for a four-dimensional torus³ [22], it is impossible to find a local gauge-fixing condition that selects a single representative per orbit. The condition (2.17) alone defines the transverse hyperplane of configurations:

$$\Gamma \equiv \{A : \partial^\mu A_\mu = 0\}. \quad (2.21)$$

Gribov suggested modifying the condition (2.17) further restricting this region to the *Gribov's Region*, using the Faddeev-Popov operator $M[A; x, y]$ [20]:

$$\Omega = \{A \in \Gamma : M[A]^{ab} \geq 0\}, \quad M[A; x, y]^{ab} = \frac{\delta F[A^G; x]^a}{\delta G^b(y)} = -\partial^\mu D_\mu^{ab}[A]. \quad (2.22)$$

However, this region is still not exempt from Gribov Copies [9, 23], implying that we need to provide an additional condition. This motivates the definition of the *fundamental modular region* Λ :

$$\Lambda = \{A \in \Omega : A = \min F_A[G]\}, \quad F_A[G] = \int d^4x \sum_\mu \text{Tr} \{A_\mu^G(x) A_\mu^G(x)\} \quad (2.23)$$

where only absolute minima are considered. The fundamental modular region Λ is free of Gribov Copies. Each gauge orbit has a single representative in the interior of Λ [24, 25]. This choice of gauge is often called *Minimal Landau Gauge*. It should be noted that the Gribov's region contains all the minima (global or local) of $F_A[G]$ whereas Λ only contains the absolute minima.

2.3 Regularization and Renormalization

When computing the Green's functions (2.11), one often ends with a divergent expression. Loop diagrams contain integrations in momentum space, which for most theories diverge (ultraviolet divergences). To circumvent this issue, a *regularization* procedure followed by *renormalization* is performed.

2.3.1 Regularization

Regularization consists in isolating the divergences of the theory using a regulator. This allows for the identification of the type of divergence of the theory. At the perturbative regime, many regularization schemes may be used such as Dimensional Regularization or

³which would correspond to our use case, an Euclidian theory with periodic boundary conditions.

the Pauli-Villars Regularization. For the non-perturbative regime, a widely used regularization scheme is the Lattice Regularization, which is the scheme in this work. This scheme is covered in chapter 3.

2.3.2 Renormalization

Once the theory is regularized, renormalization may take place by adding *counter-terms* to the Lagrangian density that effectively cancel our these divergences, while keeping the overall form of the Lagrangian unchanged which allows for the conservation of the dynamics of the theory. Since the overall form of the Lagrangian is preserved, the renormalization procedure is equivalent to a multiplicative rescaling of the fields. A possible effective Lagrangian is given by [26]:

$$\begin{aligned} \mathcal{L}_{\text{eff}}^r = & Z_3 \frac{1}{2} A_\mu^a \left(-\partial^2 \delta_{\mu\nu} - \left(\frac{1}{Z_3 \xi_r} - 1 \right) \partial_\mu \partial_\nu \right) A_\nu^a \\ & + \tilde{Z}_3 \bar{c}^a \partial^2 c^a + \tilde{Z}_1 g_r f^{abc} \bar{c}^a \partial_\mu \left(A_\mu^c c^b \right) - Z_1 g_r f^{abc} \left(\partial_\mu A_\nu^a \right) A_\mu^b A_\nu^c \\ & + Z_4 \frac{1}{4} g_r^2 f^{abe} f^{cde} A_\mu^a A_\nu^b A_\mu^c A_\nu^d + Z_2 \bar{\psi} \left(-\gamma_\mu \partial_\mu + Z_m m_r \right) \psi \\ & - Z_{1F} i g_r \bar{\psi} \gamma_\mu T^a \psi A_\mu^a. \end{aligned}$$

Where the multiplicative factors are related by:

$$Z_g g_r = g_0 \quad Z_{1F} = Z_g Z_2 Z_3^{\frac{1}{2}}, \quad Z_1 = Z_g Z_3^{\frac{3}{2}}, \quad \tilde{Z}_1 = Z_g \tilde{Z}_3 Z_3^{\frac{1}{2}}, \quad Z_4 = Z_g^2 Z_3^2. \quad (2.24)$$

These relations can be derived from the Slavnov-Taylor identities [26]. The renormalized Green's functions are equal to the unrenormalized ones with a multiplicative Z factor:

$$\langle 0 | T(\phi_1(x_1) \cdots \phi_n(x_n)) | 0 \rangle_R = Z \cdot \langle 0 | T(\phi_1(x_1) \cdots \phi_n(x_n)) | 0 \rangle. \quad (2.25)$$

The determination of the Z factors requires a choice of a renormalization scheme. Among the most used examples are the Minimal Subtraction scheme (MS) and the MOMentum space subtraction (MOM). The former defines the Z factors in such a way that the counter-terms introduced cancel out only the pole part of the respective propagators and vertices whereas the former sets the renormalized 2-point and 3-point Green's functions to be equal to its tree-level form at a given momentum value μ^2 [27]. An example of this is the determination of Z_3 for the gluon propagator:

$$D_R(\mu^2, \mu^2) = Z_3(\mu^2) D(\mu^2) = \frac{1}{\mu^2}, \quad D_{\mu\nu}^{ab}(p^2) = \delta^{ab} D(p^2) \left(g_{\mu\nu} + (\xi - 1) \frac{p^\mu p^\nu}{p^2} \right) \quad (2.26)$$

where $D_{\mu\nu}^{ab}(p^2)$ is the Green's function for the gluon propagator in momentum space and $D(p^2)$ is the corresponding form factor. Note that an extra dependence on the renormalization point μ^2 was added to the renormalized propagator $D_R(p^2, \mu^2)$.

3 Kugo Ojima Confinement Scenario

Following the Faddeev-Popov procedure, the effective Lagrangian Density of the theory (2.20) contains the ghost fields. It is known that these fields have the wrong spin-statistics relations [19]. These fields represent unphysical states, and should not contribute to the physical content of the theory (such as scattering amplitudes). Furthermore, it has not been observed an asymptotic free colored state (e.g. free quarks or gluons). This all suggests that there must exist a confinement mechanism that prevents these states to contribute to the S-matrix. While formulating the canonical formalism of non-Abelian gauge theories, Taichiro Kugo and Izumi Ojima [5] provided an hypothesis to such mechanism and it is the theme of this chapter. We will present only the key details, the full treatment can be found in [5, 28].

3.1 Preliminary Properties

In order to discuss the Kugo-Ojima confinement scenario, it is convenient to switch temporarily to the canonical formalism. Additionally, the auxiliary hermitian fields (also called the Nakanishi-Lautrup auxiliary fields¹) B^a are introduced in the theory by changing the gauge fixing term into:

$$\mathcal{L}_{GF} = \frac{\xi}{2}(B^a)^2 - B^a \partial^\mu A_\mu^a. \quad (3.1)$$

The introduction of the auxiliary fields B^a do not change the dynamics since no new degrees of freedom are introduced with their addition. It is also important to redefine the anti-ghost as [5]:

$$\bar{c}^a \longrightarrow i\bar{c}^a \implies (c^a)^\dagger = c^a, \quad (\bar{c}^a)^\dagger = \bar{c}^a \quad (3.2)$$

¹The auxiliary fields B^a originally appeared as a consistent way to perform canonical quantization of electromagnetism in the Landau gauge [29].

which implies that the Faddeev-Popov term is also changed to:

$$\mathcal{L}_{FP} = i\bar{c}^a \partial^\mu (D_\mu c)^a \quad (3.3)$$

so that the overall Lagrangian has the following form:

$$\begin{aligned} \mathcal{L}_{\text{eff}} = & -\frac{1}{4}(F^a)^{\mu\nu}(F^a)_{\mu\nu} + \sum_f \bar{\psi}_f (i\gamma^\mu \nabla_\mu - m_f)\psi_f + \\ & + \frac{\xi}{2} (B^a)^2 - B^a \partial^\mu A_\mu^a + i\bar{c}^a \partial^\mu (D_\mu c)^a. \end{aligned} \quad (3.4)$$

The canonical conjugate momenta are:

$$\begin{aligned} \pi_B^a &= \frac{\partial \mathcal{L}_{\text{eff}}}{\partial \dot{B}^a} = -A_0^a, & \pi_{A_k}^a &= \frac{\partial \mathcal{L}_{\text{eff}}}{\partial \dot{A}_k^a} = F_{0k}^a, & \pi_c^a &= \frac{\partial}{\partial \dot{c}^a} \mathcal{L}_{\text{eff}} = i\dot{\bar{c}}^a. \\ \pi_{\bar{c}}^a &= \frac{\partial}{\partial \dot{\bar{c}}^a} \mathcal{L}_{\text{eff}} = -i(\dot{c} + g f^{abc} A_0^b c^c), & \pi_\psi &= \frac{\partial}{\partial \dot{\psi}} \mathcal{L}_{\text{eff}} = \bar{\psi}(i\gamma^0). \end{aligned} \quad (3.5)$$

Note that for Grassmann variables, we adopt the left derivative definition. Having the canonical conjugate momenta defined, we can establish the usual (equal time) commutation relations:

$$\begin{aligned} [\pi_\Phi^I(x), \Phi_J(y)]_{\pm, x_0=y_0} &= -i\delta_J^I \delta(\mathbf{x} - \mathbf{y}), \\ [\Phi_I(x), \Phi_J(y)]_{\pm, x_0=y_0} &= [\pi_\Phi^I(x), \pi_\Phi^J(y)]_{\pm, x_0=y_0} = 0 \end{aligned} \quad (3.6)$$

where $\Phi_I = (B^a, A_k^a, c^a, \bar{c}^a, \psi^a)$ and π_Φ^I denote the respective conjugate momenta, by the same order. The new gauge fixing term (3.1) spoils the local gauge invariance, but it is possible to identify a generalized gauge transformation that leaves \mathcal{L}_{eff} unchanged, the BRST transformation [6, 7] such that:

$$\begin{aligned} \delta A_\mu^a &= \lambda(D_\mu c^a), & \delta c^a &= -\frac{\lambda}{2} f^{abc} c^b c^c, & \delta \bar{c}^a &= i\lambda(B^a), \\ \delta \psi^a &= i\lambda(t^c)^{ab} c^c \psi^b, & \delta B^a &= 0 \end{aligned} \quad (3.7)$$

where λ is an anticommuting constant (Grassman variable). The transformation law for a given field Φ is:

$$\begin{aligned} \Phi &\longrightarrow \Phi' = \Phi + \delta\Phi, \\ \Phi &= \{A_\mu^a, c^a, \bar{c}^a, \psi^a, \bar{\psi}^a\}. \end{aligned} \quad (3.8)$$

This transformation allows us to write the respective conserved Noether current $(J_B)_\mu$ [5], which can be rewritten using the equations of motion as:

$$(J_B)_\mu = \sum_{\Phi_I} \delta\Phi_I \frac{\partial \mathcal{L}}{\partial(\partial_\mu \Phi_I)} = B^a D_\mu c^a - (\partial_\mu B^a) c^a + \frac{i}{2} g (\partial_\mu \bar{c}^a) f^{abc} c^b c^c - \partial^\nu (F_{\mu\nu}^a c^a) \quad (3.9)$$

from which the respective conserved charge can be derived:

$$Q_B = \int d^3x (J_B)_0(x) = \int d^3x \left[B^a (D_0 c)^a - \dot{B}^a c^a + \frac{i}{2} g \dot{\bar{c}}^a f^{abc} c^b c^c \right] \quad (3.10)$$

$$\implies Q_B^\dagger = Q_B.$$

This charge generates the BRST transformation:

$$[iQ_B, \Phi]_\pm = \delta\Phi \quad (3.11)$$

where the commutation (anti-commutator) should be taken if Φ has a even (odd) number of ghost fields². Using this fact, a very important relation regarding Q_B can be derived:

$$\{Q_B, Q_B\} = 2Q_B^2 = 0 \quad (3.12)$$

in other words, the BRST-charge is nilpotent. This nilpotency of Q_B will be relevant for the confinement mechanism that we will see later. Additionally, the new hermitian assignment of the ghost fields allows the identification of a scale symmetry [5]:

$$\begin{aligned} c^a &\longrightarrow e^\theta c^a, \\ \bar{c}^a &\longrightarrow e^{-\theta} \bar{c}^a \end{aligned} \quad (3.13)$$

which has its own charge as well, the FP-charge:

$$Q_c = i \int d^3x \left(\bar{c}^a (D_0 c)^a - \dot{\bar{c}}^a c^a \right) = Q_c^\dagger. \quad (3.14)$$

Computing the commutation relations between the conserved FP-charge and the ghost fields yields:

$$\begin{aligned} [iQ_c, c^a(x)] &= c^a(x), \\ [iQ_c, \bar{c}^a(x)] &= -\bar{c}^a(x) \end{aligned} \quad (3.15)$$

These relations can be verified using the canonical commutation relation for the ghost fields. Additionally, this shows iQ_c has integer eigenvalues³. The eigenvalue of iQ_c is defined as the *FP-Ghost number* $N_{FP} \in \mathbf{Z}$.

²Due to the fermionic nature of ghost fields.

³While this may be surprising, it is consistent with the indefinite metric of the state space \mathcal{V} . Let:

$$\begin{aligned} \hat{A}^\dagger = \hat{A}, \quad \hat{A} | \alpha_n \rangle &= a_n | \alpha_n \rangle \implies \\ \langle \alpha_m | \hat{A} - \hat{A}^\dagger | \alpha_n \rangle &= (a_m^* - a_n) \langle \alpha_m | \alpha_n \rangle = 0 \end{aligned} \quad (3.16)$$

For $n = m$, $\langle \alpha_n | \alpha_n \rangle$ does not need to be strictly positive. So, we can't draw the conclusion that $a_n^* = a_n$, which means in general that the eigenvalues of an Hermitian operator can be complex. Furthermore, (3.16) implies that the eigenvalues of a hermitian operator appear in pairs conjugate of one another.

3.2 Defining the Hilbert Space

The quantization of gauge theories in covariant gauges requires considering an indefinite metric (i.e negative norm states) in the state vector space \mathcal{V} [28]. The existence of negative norms prevents us from interpreting inner products as probability amplitudes. Only when restricting \mathcal{V} to a physical subspace $\mathcal{V}_{\text{phys}} \subseteq \mathcal{V}$, a Hilbert space with positive definite metric can be defined, enabling us to recover the usual probabilistic interpretation of Quantum Mechanics⁴. To define such space, we require that [5]:

1. The Hamiltonian of the theory H is hermitian: $H^\dagger = H$;
2. The physical subspace $\mathcal{V}_{\text{phys}}$ is invariant under time development;
3. The inner product in $\mathcal{V}_{\text{phys}}$ is positive semi-definite.

Should these requirements be satisfied, a valid quantum theory, with a physical S-matrix may be formulated on the following quotient space:

$$\mathcal{H}_{\text{phys}} \equiv \mathcal{V}_{\text{phys}}/\mathcal{V}_0 \tag{3.17}$$

where \mathcal{V}_0 is the zero-norm subspace of $\mathcal{V}_{\text{phys}}$:

$$\mathcal{V}_0 = \{|\psi\rangle \in \mathcal{V}_{\text{phys}} : \langle\psi | \psi\rangle = 0\} \tag{3.18}$$

Taking the quotient space as in (3.17) allows for the definition of a space with a positive-definite inner product where the only zero-norm vector is the null vector. It is relevant to note the first and second condition may be stated in terms of the S -matrix:

1. $S^\dagger S = S S^\dagger = 1$ (Unitary S-Matrix);
2. $S\mathcal{V}_{\text{phys}} = S^{-1}\mathcal{V}_{\text{phys}} = \mathcal{V}_{\text{phys}}$.

The anti-ghost redefinition in (3.2) is vital to the first requirement, since it allows for $\mathcal{L}^\dagger = \mathcal{L} \implies H^\dagger = H$.

⁴The Gupta-Bleuler quantization [3, 4] of QED is a known example of this.

3.2.1 Physical Subspace and BRST-Algebra

To specify the physical subspace, Kugo and Ojima [5] proposed the following subsidiary condition:

$$\mathcal{V}_{\text{phys}} \equiv \ker Q_B = \{|\psi\rangle \in \mathcal{V} : Q_B|\psi\rangle = 0\} \quad (3.19)$$

Under the assumption that Q_B is unbroken⁵, this definition of the physical subspace immediately satisfies the second requirement in section 3.2, as the charge is a conserved scalar quantity, making $\mathcal{V}_{\text{phys}}$ Poincaré invariant (and in particular, invariant under time translations). Using the equal-time commutation relations (3.6) and the transformation law (3.11), we can derive the algebra between the two conserved charges we've defined so far:

$$\begin{aligned} \{Q_B, Q_B\} &= 2Q_B^2 = 0; \\ [iQ_c, Q_B] &= Q_B; \\ [Q_c, Q_c] &= 0. \end{aligned} \quad (3.20)$$

The first equation expresses the already mentioned nilpotency of Q_B . The second equation expresses an important fact: Q_B changes the FP-ghost number N_{FP} by one.

3.2.2 Inner Product Structure

Finally, the positivity of the physical subspace $\mathcal{V}_{\text{phys}}$, the third requirement mentioned in section 3.2 can be discussed. Using the BRST-algebra some features regarding the inner product can be derived: since Q_c has imaginary eigenvalues while being a hermitian operator⁶, in \mathcal{V} rise orthogonality conditions such as:

$$\langle k', N'_{FP} | k, N_{FP} \rangle \propto \delta_{N_{FP}, -N'_{FP}} \quad (3.21)$$

where k and k' refer to other relevant quantum numbers. The states $|k, N_{FP}\rangle$ and $|k, -N_{FP}\rangle$ are referred as *FP-Conjugates* of each other. The existence of a nilpotent operator such as (3.12) splits the whole state space \mathcal{V} into the following [5]:

⁵An unbroken generator of symmetry annihilates the vacuum, $Q_B|0\rangle = 0$, so that the generated symmetry is not spontaneously broken. An equivalent statement is that the charge Q_B is well-defined. This is desirable so that the BRST-Symmetry remains a global symmetry of the Lagrangian.

⁶See footnote in the previous page.

1. **BRST-Singlets:** States $|\psi\rangle$ belonging to $\mathcal{V}_{\text{phys}}$ (i.e $Q_B|\psi\rangle = 0$) such that there is no state $|\phi\rangle$ in \mathcal{V} satisfying $Q_B|\psi\rangle = |\phi\rangle$. Using the FP-Ghost number, it is possible to divide these into:
 - Physical States - BRS-Singlet with $N_{FP} = 0$;
 - Paired Singlet ($N_{FP} \neq 0$) - States that are FP-Conjugate of each other.
2. **BRST-Doublets:** Pair of states ($|\psi\rangle, |\phi\rangle$) that are related by $Q_B|\psi\rangle = |\phi\rangle$. The state $|\phi\rangle$ is called a *daughter* state whose *parent* is $|\psi\rangle$. The corresponding FP-Conjugate of these pairs form another doublet, the set of these 4 states constitutes the *quartet*.

It is possible then to draw the following conclusions:

1. The paired singlets are excluded since the existence of such states would spoil the norm-positivity in $\mathcal{V}_{\text{phys}}$. The BRST-algebra alone is not enough to exclude the existence of these states, which is why this requirement is theory-dependent. Fortunately, there is evidence to support their absence in gauge theories [5].
2. A *daughter* state $|\phi\rangle = Q_B|\psi\rangle$ belongs to the zero-norm subspace (3.18), but is also orthogonal to all other states in $\mathcal{V}_{\text{phys}}$:

$$\begin{aligned}
\langle\phi|\phi\rangle &= \langle\psi|Q_B^2|\psi\rangle = 0 \\
\langle f|\phi\rangle &= (\langle f|Q_B)|\psi\rangle = 0, \quad |f\rangle \in \mathcal{V}_{\text{phys}}
\end{aligned}
\tag{3.22}$$

3.2.3 The Quartet Mechanism

The nilpotency of Q_B has split the state vector space \mathcal{V} into singlets and quartets. Kugo and Ojima [5] have proven in a general basis the *quartet mechanism*: states belonging to quartets are confined in the physical subspace $\mathcal{V}_{\text{phys}}$. Namely, given a quartet such as:

$$\begin{aligned}
|k, N_{FP}\rangle &= \chi_k^\dagger|0\rangle \equiv |\chi_k\rangle & |k - N_{FP}\rangle &= -\beta_k^\dagger|0\rangle \equiv -|\beta_k\rangle \\
|k, N_{FP} + 1\rangle &= -i\gamma_k^\dagger|0\rangle \equiv -i|\gamma_k\rangle & |k, -N_{FP} - 1\rangle &= -\bar{\gamma}_k^\dagger|0\rangle \equiv -|\bar{\gamma}_k\rangle
\end{aligned}
\tag{3.23}$$

where

$$|\gamma_k\rangle = -iQ_B|\chi_k\rangle, \quad |\beta_k\rangle = Q_B|\bar{\gamma}_k\rangle
\tag{3.24}$$

and the corresponding quartet projector⁷:

$$P^{(n)} = \left(\frac{1}{n}\right) \sum_k \left\{ -\beta_k^\dagger P^{(n-1)} \chi_k - \chi_k^\dagger P^{(n-1)} \beta_k - \sum_j \left(\omega_{jk} \beta_k^\dagger P^{(n-1)} \beta_j \right) + \right. \\ \left. + i\gamma_k^\dagger P^{(n-1)} \bar{\gamma}_k - i\bar{\gamma}_k^\dagger P^{(n-1)} \gamma_k \right\}. \quad (3.25)$$

where $\omega_{jk} = [\chi_j, \chi_k]_\pm$, it is possible to re-write (3.25) as [5]:

$$P^{(n)} = \{iQ_B, R^{(n)}\} \quad \text{for } n \geq 1, \\ R^{(n)} \equiv i\frac{1}{n} \sum_k \left(\bar{\gamma}_k^\dagger P^{(n-1)} \chi_k + \chi_k^\dagger P^{(n-1)} \bar{\gamma}_k + \sum_j \omega_{jk} \beta_k^\dagger P^{(n-1)} \bar{\gamma}_j \right). \quad (3.26)$$

Written in this form, for any two states $|f\rangle, |g\rangle \in \mathcal{V}_{\text{phys}}$:

$$\langle f|P^{(n)}|g\rangle = 0 \quad n \geq 1. \quad (3.27)$$

So, quartet members do not contribute to the inner product defined in $\mathcal{V}_{\text{phys}}$, effectively confining these states. The recursive definition for the quartet projector in (3.25) proves this for multi-particle states. So, as long the singlet states have positive norm, the quotient space:

$$\mathcal{H}_{\text{phys}} = \mathcal{V}_{\text{phys}}/\mathcal{V}_0 \quad (3.28)$$

is a valid Hilbert space to formulate our quantum theory, satisfying the third requirement⁸ in section 3.2. The same result applies by linearity for field operators built with the creation and annihilation operators given in (3.23). Note however some assumptions must be made if this classification is to hold at the asymptotic level⁹. The BRST-transformation law (3.7) allows for the identification of the *elementary* quartet. Indeed:

$$[iQ_B, A_\mu^a]|0\rangle = Q_B (iA_\mu^a|0\rangle) = (D_\mu c)^a |0\rangle, \\ \{iQ_B, \bar{c}^a\}|0\rangle = Q_B (i\bar{c}^a|0\rangle) = iB^a|0\rangle. \quad (3.29)$$

In the case of Yang-Mills theory without spontaneous symmetry breaking, it is possible to prove [5] that asymptotically, the longitudinal and scalar polarizations of the gauge field A_μ^a along with the ghost and anti-ghost c^a, \bar{c}^a belong to the same quartet. The transverse modes are identified as physical states with positive norm. This implies that, for this theory, the positivity requirement is satisfied.

⁷For $n = 0$, $P^{(0)}$ is defined to project the singlet components.

⁸Note that, however, that this is only the case if the paired singlets mentioned in section 3.2.2 can be excluded. Additionally, we assume that the singlets with $N_{FP} = 0$, that we wish to use as representatives as physical states, have positive norm.

⁹See Appendix C of [5] for the necessary assumptions.

3.3 Color Confinement

The Lagrangian Density (2.20) is no longer gauge invariant under Local SU(3) transformations (2.8). However, it is still invariant under the global version of the transformation. Therefore, the corresponding conserved *color current* [30, 5] can be derived:

$$J_\mu^a = (A^\nu \times F_{\mu\nu})^a + j_\mu^a + (A_\mu \times B)^a - i(\bar{c} \times (D_\mu c))^a + i(\partial_\mu \bar{c} \times c)^a \quad (3.30)$$

Which allows to re-write the equation of motion of A_μ [30]:

$$gJ_\mu^a = \partial^\nu F_{\mu\nu}^a + \{Q_B, D_\mu \bar{c}^a\} \quad (3.31)$$

The corresponding charge is written as:

$$Q^a = \frac{1}{g} (G^a + N^a) \quad (3.32)$$

where

$$\begin{aligned} G^a &= \int d^3x \mathcal{G}_0^a(x), & \mathcal{G}_\mu^a(x) &= \partial^\nu F_{\mu\nu}^a(x) \\ N^a &= \int d^3x \mathcal{N}_0^a(x), & \mathcal{N}_\mu^a &= \{Q_B, (D_\mu \bar{c})^a(x)\} \end{aligned} \quad (3.33)$$

Color confinement takes place in $\mathcal{H}_{\text{phys}}$ if:

$$\langle f|Q^a|g\rangle = 0, \quad |f\rangle, |g\rangle \in \mathcal{V}_{\text{phys}} \quad (3.34)$$

Note that N^a vanishes¹⁰ in the physical subspace $\mathcal{V}_{\text{phys}}$ defined by (3.17). We will need to state the following equivalence between different statements of the Goldstone Theorem [5]: Let Q be a conserved charge of a global conserved current J_μ . Then the following statements are equivalent:

1. Q is a well-defined charge (i.e annihilates the vacuum $Q|0\rangle = 0$);
2. J_μ has no discrete massless spectrum (i.e $\langle 0|J_\mu|\Psi(p^2 = 0)\rangle = 0$);
3. Q remains unbroken (no spontaneous symmetry breaking).

We assume the well-definedness of the color charge Q^a , so that the color symmetry is not-spontaneously broken. Let's start by looking at the charges N^a as we will try to prove its well-definedness using the second statement above. We consider an arbitrary

¹⁰If the corresponding charge is well-defined, otherwise the integrations in (3.33) would be ill-defined.

linear combination of the type $N_\alpha = \alpha^a N^a$. To verify the existence or not of a massless spectrum we search for states satisfying:

$$\langle 0 | \alpha^a \mathcal{N}_\mu^a(x) | \Psi(p^2 = 0) \rangle = \alpha^a \langle 0 | \{ Q_B, (D_\mu \bar{c})^a(x) \} | \Psi(p^2 = 0) \rangle \neq 0 \quad (3.35)$$

The only non-vanishing matrix element is given by choosing $|\Psi\rangle$ to be a state created by the gauge field A_μ^a , it is possible to evaluate the inner product above to [5]:

$$\begin{aligned} \langle 0 | \alpha^a \mathcal{N}_\mu^a(x) | \Psi(p^2 = 0) \rangle &= \alpha^a \langle 0 | \{ Q_B, (D_\mu \bar{c})^a(x) \} | \Psi(p^2 = 0) \rangle = \\ &= \alpha^a (\delta^{ab} + u^{ab}) \partial_\mu D^{(+)}(x - y) \end{aligned} \quad (3.36)$$

where $D^{(+)}$ is the positive frequency part of the massless Pauli-Jordan function:

$$D^{(+)}(x - y) = -i \int \frac{d^4 p}{(2\pi)^3} \delta(p^2) e^{-ip(x-y)} \quad (3.37)$$

and the parameters u^{ab} can be calculated with the following relation [5]:

$$\int d^4 x e^{ip(x-y)} \langle 0 | T \{ (D_\mu c)^b(x) g (A_\nu \times \bar{c})^a(y) \} | 0 \rangle = -u^{ab} \frac{p_\mu p_\nu}{p^2} + \dots \quad (3.38)$$

The dots denote terms that are not relevant to the pole structure of the equation. Regarding the charges G^a , due to the anti-symmetry of $F_{\mu\nu}^a$ it can be shown (Chapter 6, Lemma 6.1 of [5]) that if the linear combination of these charges $G_\alpha = \alpha^a G^a$ is well-defined, then it must vanish (i.e $G_\alpha = 0$). Now, if

$$u^{ab}(p^2 = 0) = -\delta^{ab} \quad (3.39)$$

is satisfied, then the charges N_α are well-defined, but since Q_α is assumed to be well-defined, then G_α has to be as well and in turn means that it vanishes $G_\alpha = 0$. This leaves the following definition for the color charge Q_α :

$$Q_\alpha = \frac{1}{g} (G_\alpha + N_\alpha) = \frac{1}{g} N_\alpha = \frac{\alpha^a}{g} \int d^3 x \{ Q_B, (D_0 \bar{c})^a(x) \}. \quad (3.40)$$

As previously stated before, if the charge N_α is well-defined, it vanishes in the physical subspace $\mathcal{V}_{\text{phys}}$ which, according to the previous equation, applies as well to the color charge Q_α . Consequently, all states in the physical subspace $\mathcal{V}_{\text{phys}}$ (and consequently in $\mathcal{H}_{\text{phys}}$) are colorless, and color confinement (3.34) takes place:

$$\langle f | Q_\alpha | g \rangle = 0, \quad |f\rangle, |g\rangle \in \mathcal{V}_{\text{phys}} \quad (3.41)$$

So, the conditions for color confinement in $\mathcal{H}_{\text{phys}}$ come as:

1. $u^{ab}(p^2 = 0) = -\delta^{ab}$;
2. the color charge Q^a remains an unbroken generator of symmetry;

then color confinement (3.41) takes place in $\mathcal{H}_{\text{phys}}$. Since the color symmetry is assumed to remain unbroken, the second condition is automatically satisfied. The first condition can be studied using (3.38) to obtain $u^{ab}(p^2)$. In the Landau gauge, the condition (2.17) translates to $p^\mu A_\mu(p) = 0$ in momentum space, which in turns means that this function is transverse in the Lorentz space, allowing to write:

$$\int d^4x e^{ip(x-y)} \langle 0|T \left((D_\mu c)^b(x) g (A_\nu \times \bar{c})^a(y) \right) |0\rangle \equiv \mathcal{U}_{\mu\nu}^{ab} = (P_T)_{\mu\nu}(p) u^{ab}(p^2) \quad (3.42)$$

where $(P_T)_{\mu\nu}(p) = \left(\delta_{\mu\nu} - \frac{p_\mu p_\nu}{p^2} \right)$. Following equation (3.42), contracting both sides with the transversal projector yields u^{ab} :

$$(P_T)^{\mu\nu}(p) \mathcal{U}_{\mu\nu}^{ab}(p) = (N_d - 1) u^{ab}(p^2). \quad (3.43)$$

Where N_d is the dimension of the space-time considered. Finally, it is expected that $u^{ab}(p^2)$ is diagonal in colour space:

$$u^{ab}(p^2) = u(p^2) \delta^{ab} \quad (3.44)$$

From equation (3.42), contracting the right-hand side of the equation with the longitudinal projector $(P_L)^{\mu\nu}(p) = p^\mu p^\nu / p^2$ yields zero. Taking into consideration this with (3.43) and (3.44), the function $u(p^2)$ may be obtained taking the trace in both color and Lorentz spaces:

$$u(p^2) = \frac{1}{(N_d - 1)(N^2 - 1)} \sum_{a,\mu} \mathcal{U}_{\mu\mu}^{aa}(p) \quad (3.45)$$

The factor $N^2 - 1$ is the dimension of the SU(N) Lie Algebra. Since, in our case, the gauge group is SU(3), this factor comes as $N^2 - 1 = 8$. We are also considering a four-dimensional space-time $N_d = 4$. The confinement criterion specified before (3.3) translates into:

$$\lim_{p^2 \rightarrow 0} u(p^2) = -1 \quad (3.46)$$

4 Lattice Computation of the Kugo-Ojima function

In this chapter, the methodology of the computation of the Kugo-Ojima function (3.38) on the lattice is discussed. This chapter starts by presenting the details regarding the lattice formulation of Gauge Theories. As mentioned in section 2.3.1, this formulation provides a method to regularize non-perturbatively gauge theories. The basic formulas are presented along with the key details that allow for the simulation of gauge theories in the computer. Using the lattice formulation of gauge theories, we present the lattice gauge-fixing procedure and discuss the use of Monte-Carlo methods to extract quantities of interest. Finally, the lattice computation of the Kugo-Ojima function is discussed, as well as some of its properties.

4.1 Lattice Discretization

The first step is to discretize the Euclidean space-time into a hypercubic lattice:

$$x_\mu = an_\mu, n_\mu \in \{0, \dots, N(\mu) - 1\}. \quad (4.1)$$

The parameter a is the *lattice spacing* and $N(\mu)$ is the number of sites of the lattice in the μ direction¹. This directly imposes a momentum cut-off in our theory. To see this, let's start by noting that:

$$\exp\{ip_\mu x^\mu\} = \exp\{i(p^\mu x_\mu + 2\pi n_\mu)\} = \exp\left\{ix_\mu \left(p^\mu + \frac{2\pi}{a}\right)\right\}. \quad (4.2)$$

Looking at the Fourier transform of an arbitrary scalar function, the previous equation implies:

$$F(p) = \int d^4x e^{-ip^\mu x_\mu} f(x) \implies F\left(p + \frac{2\pi}{a}\right) = F(p) \quad (4.3)$$

¹In this work, we use only symmetric lattices, which have the same number of sites in each direction.

Therefore, momentum space integrations can be restricted to the Brillouin zone $-\frac{\pi}{a} < p_\mu \leq \frac{\pi}{a}$, effectively introducing a high-momentum regulator in the theory. This allows us to write the inverse Fourier transformation of a given lattice function $f(x)$ as:

$$f(x) = \int_{-\frac{\pi}{a}}^{\frac{\pi}{a}} \frac{d^4 p}{(2\pi)^4} F(p) e^{ip^\mu x_\mu}. \quad (4.4)$$

To perform lattice calculations on the computer, one should use a finite lattice with periodic boundary conditions. As a consequence of (4.3), the momenta on the lattice are also discretized:

$$f(x^\mu + L(\mu)\hat{\mu}) = f(x^\mu) \implies \exp\{iL(\mu)p_\mu\hat{\mu}\} = 1 \implies p_\mu = \frac{\pi}{L(\mu)}n_\mu, \quad (4.5)$$

$$n_\mu = -\frac{N(\mu)}{2} + 1, \dots, \frac{N(\mu)}{2}$$

where $L(\mu) = N(\mu)a$ and $\hat{\mu}$ is the unit vector in the μ direction:

$$\hat{\mu} \equiv e^\mu = \begin{pmatrix} \delta_0^\mu \\ \delta_1^\mu \\ \delta_2^\mu \\ \delta_3^\mu \end{pmatrix}. \quad (4.6)$$

The momentum p_μ is called the *naive momentum*. It is often found that the naive momenta is not the most adequate to describe observables on the lattice, which leads to the definition of the *improved momentum*²:

$$q_\mu = \frac{2}{a} \sin(p_\mu a). \quad (4.7)$$

4.2 Gauge Fields on the Lattice

Having the space-time discretized, it is important to know how to write relevant quantities such as the gauge fields A_μ^a . In the discrete version of the theory, these fields are replaced by the *link* variable:

$$U_\mu(x) \equiv \exp\left\{iag_0 A_\mu\left(x + \frac{a}{2}\hat{\mu}\right)\right\} \in \text{SU}(3). \quad (4.8)$$

Note how this link variable, that now takes the role of the gauge fields, are elements of the Lie group $\text{SU}(3)$ whereas the gauge fields were Lie algebra elements. The link has

²This alternative definition is motivated by calculating the propagator of a lattice regularized real scalar field theory, check Section 16.2 of reference [31].

a motivation: it is the parallel transporter between adjacent points of the lattice, see Appendix A. Using (4.8), the gauge field A_μ^a can be written as a function of the links $U_\mu(x)$:

$$A_\mu \left(x + \frac{a}{2} \hat{\mu} \right) = \frac{1}{2ig_0} [U_\mu(x) - U_\mu^\dagger(x)] - \frac{1}{6ig_0} \text{Tr} [U_\mu(x) - U_\mu^\dagger(x)] + \mathcal{O}(a^2) \quad (4.9)$$

where the second term has been included explicitly to preserve the traceless property of the gauge field A_μ . Due to its directional nature, it is possible to define the following [1]:

$$U_{-\mu}(x) \equiv U^\dagger(x - a\hat{\mu}) \quad (4.10)$$

Before continuing, note how both in (4.8) and (4.9) the argument of the gauge field A_μ^a is a point in-between two adjacent lattice points³. Another important detail is the link's gauge transformation law:

$$U_\mu^G(x) = G(x)U_\mu(x)G^\dagger(x + a\hat{\mu}). \quad (4.11)$$

The *plaquette* is defined as a product of links along the shortest possible closed path:

$$\begin{aligned} P_{\mu\nu}(x) &= U_\mu(x)U_\nu(x + a\hat{\mu})U_{-\mu}(x + a(\hat{\mu} + \hat{\nu}))U_{-\nu}(x + a\hat{\nu}) \approx \\ &\approx \exp \left\{ \left(ia^2 F_{\mu\nu}(x) \right) \right\} + \mathcal{O}(a^3). \end{aligned} \quad (4.12)$$

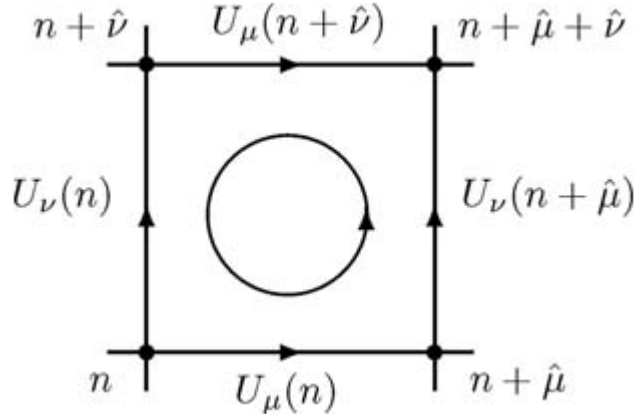


Figure 4.1: The Plaquette as a closed loop of links. The definition in (4.10) was used. Image from [1].

³In practice, we will define a 4-dimensional array of points and put 4 links in each point, one for each direction $\hat{\mu}$. Using formula (4.9) gives us the value of the gauge field in the middle of two adjacent lattice points.

Using (4.11):

$$\text{Tr} \{ P_{\mu\nu}^G(x) \} = \text{Tr} \{ P_{\mu\nu}(x) \} \quad (4.13)$$

due to the cyclic property of the trace and summing over all plaquettes, each counted with only one orientation, it is possible to define the *Wilson Gauge Action* [32]:

$$S_G[U] = \beta \sum_x \sum_{\mu < \nu} \text{Re} [\text{Tr} \{ \mathbf{1} - U_{\mu\nu}(x) \}] \quad (4.14)$$

where $\beta = \frac{2N_c}{g_0^2}$, and N_c is the number of colours ($N_c = 3$ in the case of QCD). It can be shown that this definition approximates to the Yang-Mills action in the continuum [32]:

$$S_G[U] = a^4 \frac{\beta}{4} \sum_x \sum_{\mu\nu} (F_{\mu\nu}(x))^2 + \mathcal{O}(a^2). \quad (4.15)$$

The set of links in a given lattice is called a *configuration*. The definition (4.14) is the only action used for this work, since we shall be considering only pure-gauge configurations, since the Kugo-Ojima scenario can be computed using these configurations. Some further details regarding the configurations are given in the next section.

4.3 Numerical Aspects

So far, we have discussed how to define the gluon fields on the lattice as well as how to compute the action for a given configuration. The next step, which is discussed in this section, is the calculation of quantities of interest, such as Green's functions or observables. Additionally, Green's functions depend on the gauge fixing condition so the links should also reflect the gauge fixing condition.

4.3.1 Lattice Observables

In the continuum limit, according to the Path-Integral formalism, expectation values of observables can be written as:

$$\langle \mathcal{O} \rangle = \frac{\int \mathcal{D}\phi_1 \dots \mathcal{D}\phi_n \mathcal{O}[\phi_1, \dots, \phi_n] e^{-S_G[\phi_1, \dots, \phi_n]}}{\int \mathcal{D}\phi_1 \dots \mathcal{D}\phi_n e^{-S_G[\phi_1, \dots, \phi_n]}}. \quad (4.16)$$

On the lattice, this can be written as [1]:

$$\langle \mathcal{O} \rangle = \frac{\int \mathcal{D}U \mathcal{O}[U] e^{-S_G[U]}}{\int \mathcal{D}U e^{-S_G[U]}}. \quad (4.17)$$

Numerically, it is very expensive to compute the exact functional integration in the equation above. Fortunately, Monte-Carlo simulations are ideal to compute multidimensional integrals such as these. This allows approximating the observable $\langle \mathcal{O} \rangle$ as:

$$\langle \mathcal{O} \rangle_U = \frac{1}{N} \sum_{\{U_n\}'} \mathcal{O}[U_n]. \quad (4.18)$$

where $\{U_n\}'$ is a set of configurations selected in accordance with the probability distribution given by the Boltzmann factor $P[U] \propto e^{-S_G[U]}$. The sampling process is accomplished by a *Markov chain* [1]. To estimate the uncertainty of the observables computed, we use the *bootstrap* method. This method generates N_{boot} samples, each composed of N_{sample} randomly selected values of the observable over the configurations. For the boot sample i , \mathcal{A}_i is the observable average over the selected values by that boot sample. The upper and lower limit uncertainties of a given observable are given by [1]:

$$\sigma_{up} = a^* - \langle \mathcal{A} \rangle \quad \sigma_{down} = \langle \mathcal{A} \rangle - b^* \quad (4.19)$$

where

$$\frac{\#\{\mathcal{A}_i < a^*\}}{N_{boot}} = \frac{1 - C}{2} \quad \frac{\#\{\mathcal{A}_i < b^*\}}{N_{boot}} = \frac{1 + C}{2} \quad (4.20)$$

and C is the confidence level. The standard value of C is 0.68, which we have used in this work. In this work, we also use $N_{\text{samples}} = 10N_{\text{boot}}$.

4.3.2 Gauge Fixing

The restrictions imposed on the gauge fields by the gauge fixing condition (2.16) should also be reflected on a configuration's links. Fixing the Landau gauge on the lattice is achieved by maximizing the following functional:

$$F_U[G] = A \sum_{x,\mu} \text{Re} \left\{ \text{Tr} \left[G(x) U_\mu(x) G^\dagger(x + a\hat{\mu}) \right] \right\} \quad (4.21)$$

where A is a normalization factor. The gauge transformed $U^G(x) = G(x)U(x)G^\dagger(x + a\hat{\mu})$ that maximizes the functional $F_U[G]$ is the one that satisfies (2.16). In other words:

$$\begin{aligned} \left. \frac{\delta F_U[G]}{\delta G^a(x)} \right|_{G=\tilde{G}} = 0 &\implies \partial^\mu \left(A^{\tilde{G}} \right)_\mu^a(x) = 0, \\ \left. \frac{\delta^2 F_U[G]}{\delta G^a(x) \delta G^b(y)} \right|_{G=\tilde{G}} &= -M[A; x, y]^{ab} \leq 0. \end{aligned} \quad (4.22)$$

The proof can be found in Appendix B. Similarly to the continuum version of the theory, it is possible to define the regions Γ , Ω and Λ but in terms of the configurations U :

$$\begin{aligned}\Gamma &= \{U : \partial^\mu A_\mu[U; x] = 0\}, \\ \Omega &= \{U \in \Gamma : M[U] \geq 0\}, \\ \Lambda &= \{U \in \Omega : F_U[\mathbf{I}] \geq F_U[G], \forall g \in \text{SU}(3)\}.\end{aligned}\tag{4.23}$$

Ideally, following the discussion of section 2.2.2, one would select the global maxima of (4.21), more specifically, configurations belonging to Λ . This is a highly difficult global optimization task and may require the combination of local and global optimization methods. One such combination is the CEASD⁴ method [33, 34, 35], that combines the usual Steepest Descent method [36] with an Evolutionary Algorithm. Unfortunately, deploying this method for every configuration is numerically very expensive. So, in this work, we do not consider the effect of Gribov copies, utilizing only the Steepest Descent method as a local maximization method which restricts the space of configurations to Ω . It should be noted that the effect of Gribov copies is small for the gluon and ghost propagators, normally within 1 to 2 standard deviations [37, 38].

4.4 The Lattice Kugo-Ojima function

The necessary tools of lattice gauge theories have been introduced and we can now discuss the computation of the Kugo-Ojima function (3.42) on the lattice. The lattice equivalent definition of (3.42) is given by [39]:

$$\begin{aligned}\mathcal{U}_{\mu\nu}^{ab}(p) &:= \frac{1}{V} \sum_{x,y} \sum_{c,d,e} e^{-ip \cdot (x-y)} \left\langle D_\mu^{ae} c^e(x) f^{bcd} A_\nu^d(y) \bar{c}^c(y) \right\rangle_U \\ &= \frac{1}{V} \left\langle \sum_{x,y,z} \sum_{c,d,e} e^{-ip \cdot (x-y)} (D_\mu)^{ae}(x; z) (M^{-1})^{ec}(z; y) f^{bcd} A_\nu^d(y) \right\rangle_U\end{aligned}\tag{4.24}$$

where the subscript U denotes the average over configurations. We have written explicitly all sums to be considered, dropping the repeated index convention we have been using so far. The ghost $c^e(x)$ and anti-ghost $\bar{c}^c(y)$ fields in (4.24) were replaced with the inverse of the Faddeev-Popov operator (2.23):

$$\langle 0 | \bar{c}^a(x) c^b(y) | 0 \rangle = \langle 0 | (M^{-1})^{ab}(x; y) | 0 \rangle.\tag{4.25}$$

⁴Combined Evolution Algorithm Steepest Descent.

This correspondence can be read off directly the Faddeev-Popov term in the Lagrangian density:

$$\mathcal{L}_{FP} = i\bar{c}^a \partial^\mu (D_\mu c)^a = -i\bar{c}^a M^{ab} c^b. \quad (4.26)$$

The lattice version of the Faddeev-Popov operator can be written as [40, 41]:

$$\begin{aligned} M^{ab}(x; y) = & \sum_{\mu} \text{Re} \left[\text{Tr} \left\{ t^a, t^b \right\} (U_\mu(x) + U_\mu(x - \hat{\mu})) \right] \delta_{x,y} - \\ & - 2 \sum_{\mu} \text{Re} \left[\text{Tr} \left\{ t^b t^a U_\mu(x) \right\} \right] \delta_{x+\hat{\mu},y} - 2 \sum_{\mu} \text{Re} \left[\text{Tr} \left\{ t^a t^b U_\mu(x - \hat{\mu}) \right\} \right] \delta_{x-\hat{\mu},y}. \end{aligned} \quad (4.27)$$

Similarly, the covariant derivative in the adjoint representation has the following equivalent lattice expression [42]:

$$(D_\mu[U])^{ab}(x; y) = 2 \text{Re} \left[\text{Tr} \left\{ t^b t^a U_\mu(x) \right\} \right] \delta_{x+\hat{\mu},y} - 2 \text{Re} \left[\text{Tr} \left\{ t^a t^b U_\mu(x) \right\} \right] \delta_{x,y} \quad (4.28)$$

which, up to $\mathcal{O}(a^2)$ replicates the second expression in (2.4).

4.4.1 Computational Recipe

We start out by writing the lattice definition of $\mathcal{U}_{\mu\nu}^{ab}$ as [39]:

$$\mathcal{U}_{\mu\nu}^{ab}(p) = \left\langle \sum_x e^{-ip \cdot x} [D_\mu \psi_{b,\nu}(p)]^a(x) \right\rangle_U \quad (4.29)$$

where ψ_ν^b is the solution of the system:

$$[M\psi_{b,\nu}(p)]^c(y) = \left(\sum_d f^{bcd} A_\nu^d(y) \right) e^{ip \cdot y}. \quad (4.30)$$

However, solving (4.30), requires selecting a single momenta value k to compute the inversion. This effectively means that the system must be solved for each value of k , which, for large lattices, requires a lot of computational resources to compute it in a reasonable amount of time. So, instead of inverting the system (4.30) using the full plane-wave as an extended source, we use a point-source:

$$[M\psi_{b,\nu}]^c(y) = \left(\sum_d f^{bcd} A_\nu^d(y) \right) \delta_{y,y_0}. \quad (4.31)$$

where y_0 is the coordinate of the point-source. The delta function in the previous equation fixes one of the Green's function points, effectively suppressing the sum in y . Using the solution of the system (4.31) in (4.29), we obtain [43]:

$$\left\langle \sum_{x,y,z} \sum_{c,d,e} e^{-ip \cdot x} (D_\mu)^{ae}(x; z) (M^{-1})^{ec}(z; y) (f^{bcd} A_\nu^d(y) \delta_{y,y_0}) \right\rangle_U = e^{-ip \cdot y_0} \tilde{\mathcal{U}}_{\mu\nu}^{ab}(p). \quad (4.32)$$

Note, however, that the result of this procedure is a *point-to-all* propagator ($\tilde{\mathcal{U}}_{\mu\nu}^{ab}$) instead of a *all-to-all* propagator ($\mathcal{U}_{\mu\nu}^{ab}$):

$$\begin{aligned}\tilde{\mathcal{U}}_{\mu\nu}^{ab}(p) &= e^{ip \cdot y_0} \sum_x e^{-ip \cdot x} \tilde{\mathcal{U}}_{\mu\nu}^{ab}(x - y_0), \\ \tilde{\mathcal{U}}_{\mu\nu}^{ab}(x - y) &= \sum_z \sum_{c,d,e} (D_\mu)^{ae}(x; z) (M^{-1})^{ec}(z; y) f^{bcd} A_\nu^d(y)\end{aligned}\tag{4.33}$$

If one included all possible sources in the calculation, we would re-gain the all-to-all propagator:

$$\frac{1}{V} \sum_y e^{ip \cdot y} \tilde{\mathcal{U}}_{\mu\nu}^{ab}(p) = \mathcal{U}_{\mu\nu}^{ab}(p)\tag{4.34}$$

but doing so would be very time consuming for the lattice volumes we will be considering. So, we will use the point-to-all propagator to obtain an estimative of the all-to-all propagator. Since not all points are used to compute the function, the statistical fluctuations are higher comparatively to solving (4.30). Including more sources and averaging over the result allows us to obtain a better estimative of the *all-to-all* propagator, improving the precision of the results.

The next task is to solve the system (4.31). The Conjugate-Gradient method [44] seems ideal to solve the system (4.31), as the matrix M is real and symmetric⁵. However, it is singular, since a constant vector is a null-mode of the matrix⁶. In other terms, the kernel of M is non-trivial [45]:

$$\ker M \equiv K = \left\{ \omega : \sum_{y,b} M^{ab}(x; y) \omega^b(y) = 0 \right\} \neq \{0\}.\tag{4.36}$$

as constant modes belong to this subspace. Therefore, it is only possible to invert the Faddeev-Popov matrix in the kernel's orthogonal component K^\perp . To guarantee that the solution of (4.30) converges to a unique solution in K^\perp , we instead solve the expanded system:

$$\begin{aligned}MY &= M\phi_{b,\nu} \quad \text{where} \quad \phi_{b,\nu} = \sum_d f^{bcd} A_\nu^d(y) \delta_{y,y_0} \\ M\psi_{b,\nu} &= Y.\end{aligned}\tag{4.37}$$

⁵Note that since the source used to invert the system (4.31) is real, the solution obtained by the Conjugate-Gradient method is also real.

⁶For any constant vector C_y^b , using (4.25):

$$M_{xy}^{ab} C_b^y = 0\tag{4.35}$$

As expected, since M is the discrete version of the Faddeev-Popov operator $\partial^\mu D_\mu^{ab}$.

The multiplication of $\phi_{b,\nu}$ by M in the first system guarantees that Y belongs to the orthogonal subspace⁷ K^\perp . The Conjugate-Gradient method then guarantees that a unique solution is found in K^\perp [45]. This is also valid for the second system, which analogously allows us to obtain a unique solution for $\psi_{b,\nu}$ in K^\perp . However, rounding numerical errors may destroy the orthogonality of the solution [43]. These errors can introduce null-modes back to the solution. To make sure this does not happen, we periodically remove the null-modes throughout the iterations of the Conjugate-Gradient method [43]. Consider the Fourier decomposition of a generic field $S(x)$:

$$S(x) = \sum_p c(p)e^{ip \cdot x} = c(0) + \sum_{p \neq 0} c(p)e^{ip \cdot x}. \quad (4.39)$$

Summing over x on both sides:

$$\begin{aligned} \sum_x S(x) &= \sum_x c(0) + \sum_{p \neq 0, x} c(p)e^{ip \cdot x} \iff \left(\sum_x S(x) \right) = Vc(0) + \sum_{p \neq 0} c(p)\delta_{p,0} \implies \\ &\implies c(0) = \frac{1}{V} \sum_x S(x). \end{aligned} \quad (4.40)$$

So, throughout the Conjugate-Gradient's iterations⁸, to account for the finite precision arithmetics, we subtract the null-mode to prevent the solution from escaping the orthogonal space:

$$S(x)^\perp = S(x) - \frac{1}{V} \sum_x S(x). \quad (4.41)$$

This concludes the discussion on how to solve the system in (4.31). After solving the system, we apply the lattice version of the covariant derivative (4.28), take the Fourier transform and multiply by the exponential factor $e^{ik \cdot y_0}$ just like stated in (4.32). For a given value of a, μ this method yields $\mathcal{U}_{\mu\mu}^{aa}$ (no sum intended) for all the values of p^2 with two inversions of the Faddeev-Popov matrix. This amounts to $2 \times N_d \times (N_c^2 - 1) = 2 \times 4 \times 8 = 64$ inversions required to compute the full trace.

The computation may be then summarized in the following steps:

⁷Any given color-vector $\omega = \omega^a(x)t^a$ may be decomposed into a linear combination of null-modes $\omega_0^a \in K$ and the remaining modes $\omega_1^a \in K^\perp$:

$$\omega^a = \omega_0^a + \omega_1^a \implies M(\omega^a) = M(\omega_0^a + \omega_1^a) = M\omega_1^a \neq 0 \quad (4.38)$$

So that $M\omega^a \in K^\perp$.

⁸Every 25 iterations to be exact.

1. Computation of the Kugo-Ojima source, $\phi_{b,\nu} = \sum_d f^{bcd} A_\nu^d(y) \delta_{y,y_0}$ where we use the following relation:

$$\sum_d f_{bcd} A_\nu^d(y) = -\frac{1}{2} \text{Tr} \left[\left\{ \left(U_{-\nu}^\dagger(y) + U_\nu(y) \right) - \left(U_{-\nu}^\dagger(y) + U_\nu(y) \right)^\dagger \right\} [t^b, t^c] \right]. \quad (4.42)$$

See Appendix C for full-derivation. Since we're only interested in the trace of $\mathcal{U}_{\mu\nu}^{ab}$, we set $b = a$ and $\mu = \nu$;

2. Solving the expanded system (4.37) for all the values of color index a . y_0 allows us to fix the location of the point-source⁹. We use the conjugate gradient methods with a pre-conditioner given by the operator $-\Delta^{-1} = (FT)^{-1} q^{-2}(p) (FT)$ [39], where FT denotes Fourier Transform;
3. After obtaining $\psi_{a,\mu}$ for all color and Lorentz indices, we compute the covariant derivative of the result $[D_\mu \psi_{a,\mu}]^a(x) = \sum_{b,z} (D_\mu)^{ac}(x; z) (\psi_{a,\mu})^c(z)$;
4. Taking the Fourier transform of the result and multiplying by the appropriate exponential factor yields the function for a single source, $\mathcal{U}_{\mu\mu}^{aa}(p) = e^{ip \cdot y_0} \sum_x e^{-ik \cdot x} [D_\mu \psi_{a,\mu}]^a(x)$;
5. Repeat and increment the output of the previous step for all the values of (a, μ) , which, after considering the correct normalization factors (3.45), yields the function $u(p^2)$.

Regarding software, we make use of Lattice Quantum Chromodynamics oriented libraries such as *QDP++*, *Chroma* [46, 47] and the MPI based software *PFFT* [48].

4.4.2 Longitudinal Test

An important feature of the Kugo-Ojima function is its transversality, since the Landau gauge implies that $\sum_\mu p_\mu A_\mu(p) = 0$. One should test if this property holds in the lattice version of the function, since a non-zero longitudinal component may appear from the inversion of the Faddeev-Popov matrix. A simple test is to contract the Lorentz indices with the longitudinal projector $(P_L)^{\mu\nu}(p) = \frac{p^\mu p^\nu}{p^2}$ and to see whether the result is zero:

$$(P_L)^{\mu\nu}(p) \sum_a \mathcal{U}_{\mu\nu}^{aa}(p) \equiv L(p) = 0. \quad (4.43)$$

In this work, we perform the longitudinal test for both the naive and improved momentum:

$$(P_L)^{\mu\nu}(p) = \frac{p^\mu p^\nu}{p^2} \quad \text{and} \quad (P_L)^{\mu\nu}(q) = \frac{q^\mu q^\nu}{q^2}. \quad (4.44)$$

⁹Note that $\psi_{a,\mu}$ is a color-vector defined over the lattice, i.e. $\psi_{a,\mu} \equiv (\psi_{a,\mu})^e(y)$.

4.4.3 Lattice Artifacts

As a correlation function, the Kugo-Ojima function should only depend on the magnitude of the momentum (justifying the argument p^2). In a continuum Euclidean space-time, the Kugo-Ojima function is invariant under rotations of the $O(4)$ group, which includes rotations and inversions. On the lattice, this group is broken down into the $H(4)$ group [49], discretizing the rotations into multiples of $\frac{\pi}{2}$. In other words, for a given momentum $p_\mu = (p_x, p_y, p_z, p_t)$, the Kugo-Ojima function should be invariant under permutations and sign inversions. Despite this, due to the nature of the Monte Carlo method, the computed function on the lattice will not have the same value for these equivalent momenta. So, to reduce this effect, for a given value of p^2 , we average the value of the Kugo-Ojima function over all the equivalent momenta. This is called Z4 averaging. Conversely, it is possible to prove that a polynomial scalar lattice function can be written as a function of the $H(4)$ invariants [50]:

$$\begin{aligned}
 p^{[n]} &= \sum_{\mu=1}^{N_d} p_\mu^n, \quad n = \{2, 4, 6, 8\}, \\
 u(p^2) &= \sum_a u^{aa}(p^2) \equiv u(p^{[2]}, p^{[4]}, p^{[6]}, p^{[8]}).
 \end{aligned}
 \tag{4.45}$$

In the continuum, the orbits are labeled only by the p^2 . So, assuming that we can expand the Kugo-Ojima function on the lattice as:

$$\begin{aligned}
 u(p^{[2]}, p^{[4]}, p^{[6]}, p^{[8]}) &\approx u(p^{[2]}, 0, 0, 0) + p^{[4]} \frac{\partial u}{\partial p^{[4]}}(p^{[2]}, 0, 0, 0) + \mathcal{O}(a^4) \equiv \\
 &\equiv A(p) + p^{[4]} B(p).
 \end{aligned}
 \tag{4.46}$$

we can identify $A(p)$ as the continuum version of the Kugo-Ojima function, in a finite volume. This is called the H4 method, and allows for the removal of the dependence in the higher order invariants that break the $O(4)$ invariance. Alternatively, one can use momenta points that minimize $p^{[4]}$, suppressing their contribution. These momenta points belong near the diagonal of the lattice. In this work we perform a conical cut followed by a cylindrical cut [51]. The conical cut is performed with a half-angle of 20° along the diagonal, keeping only the points that lay inside the cone. The cylindrical cut follows the same reasoning, keeping the points that lay within a cylinder with unit radius along the diagonal. Additionally, all points with $q < 0.7$ GeV are represented, and do not have to pass the previous two cuts mentioned. Although most of the results presented will be using these momentum cuts, we later compare how both methods perform.

5 Results and Discussion

In this chapter the results of the lattice computation of the Kugo-Ojima function are presented. The configurations used in this work were generated considering a 4-dimensional pure Yang-Mills action, with $\beta = 6.0 \implies a^{-1} = 1.943(47)$ GeV [52]. All the configurations were rotated to the Landau Gauge. Unless specified, all plots are represented as a function of the improved momentum q (4.7). As mentioned before, all the results are presented as bare quantities. We shall present results for 4 different symmetric lattices ($32^4, 48^4, 64^4, 80^4$). First we will present the result for the bare Kugo-Ojima function itself, which is the main goal of this work, followed by the longitudinal test mentioned in section 4.4.2. Then, some statistical considerations will be made regarding the inclusion of negative momenta, the H4 method and the statistical differences between including more configurations and more sources. Finally, a renormalization procedure is performed on the results. Below, a table with the lattice setup is presented:

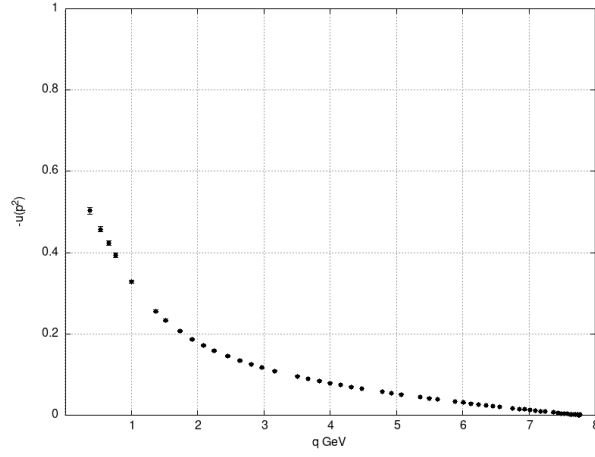
Lattice	# Configs	# Sources	β	a^{-1} (GeV)
32^4	300	6		
48^4	200	2	6.0	1.943(47)
64^4	600	1		
80^4	400	1		

Table 5.1: Configuration setup of this work.

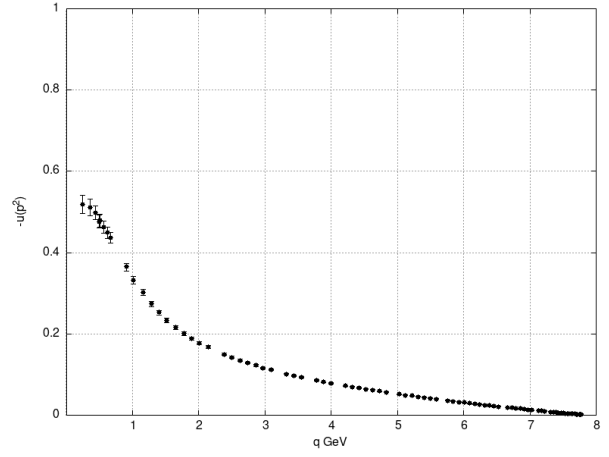
Unless specified, the presented results have the configurations referred in the table above.

5.1 The Bare Kugo-Ojima function

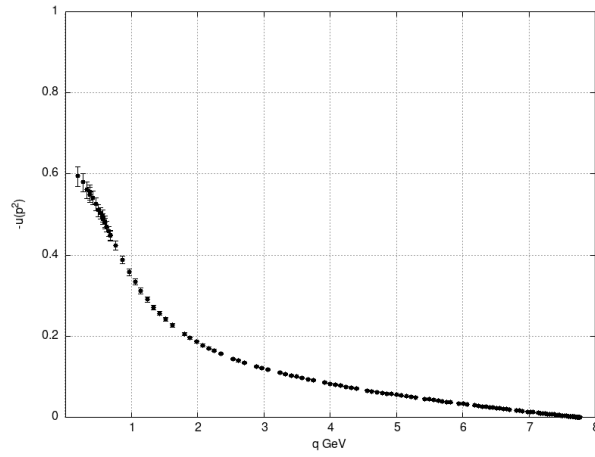
Below we present the plots for the bare Kugo-Ojima function for each lattice:



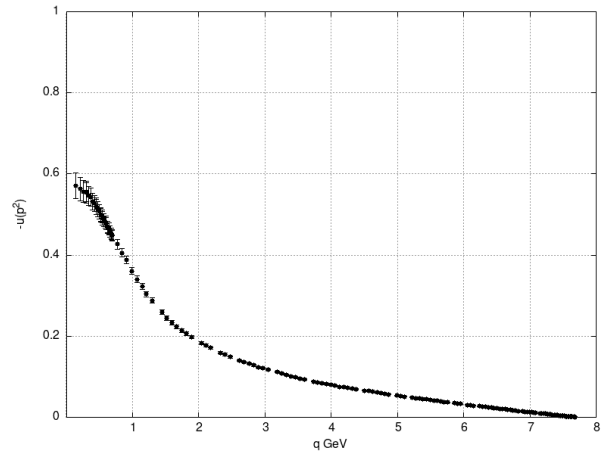
(a) 32^4 Lattice.



(b) 48^4 Lattice.



(c) 64^4 Lattice.



(d) 80^4 Lattice.

Figure 5.1: The function $u(p^2)$ for all lattice volumes.

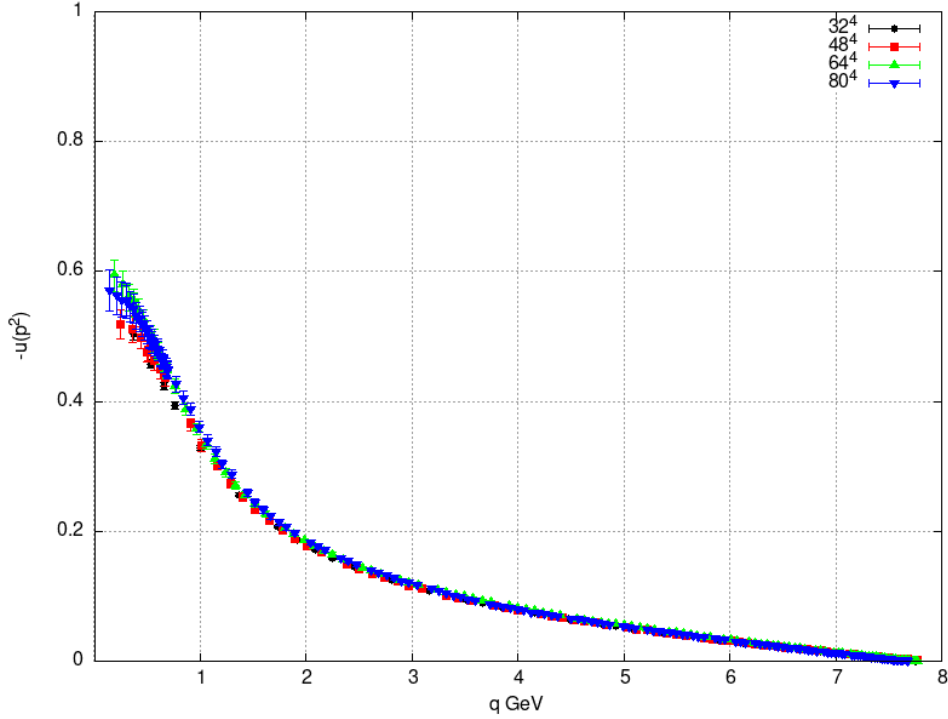


Figure 5.2: All the previous plots combined.

The first point for $p = 0$ has been excluded from the graphs, since following the null-modes discussion (4.39), it has effectively no meaning¹ [43]. As expected, the largest lattices have more momenta points in the infrared, making these the better choice to extrapolate the $p = 0$ value. It is helpful to zoom-in in the infrared region:

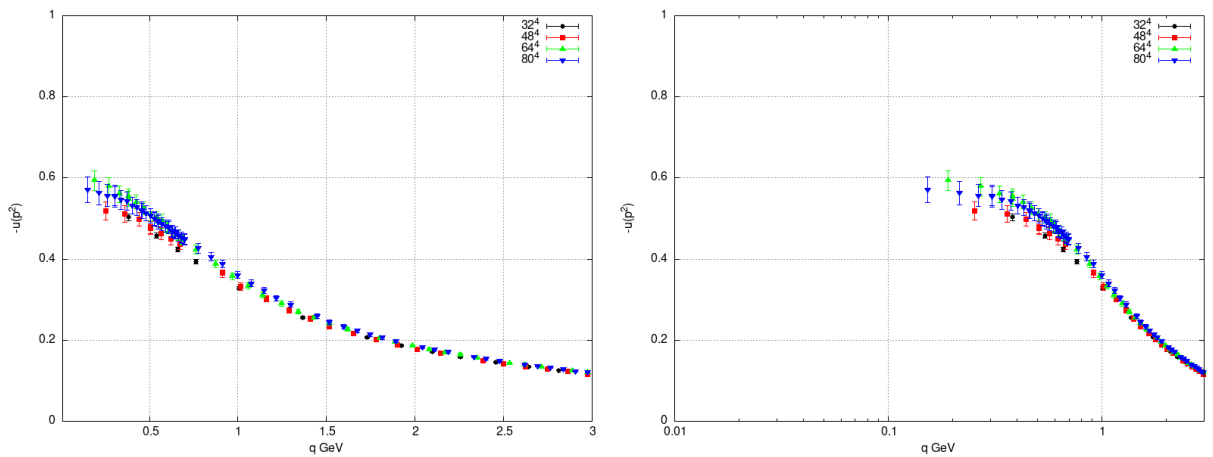


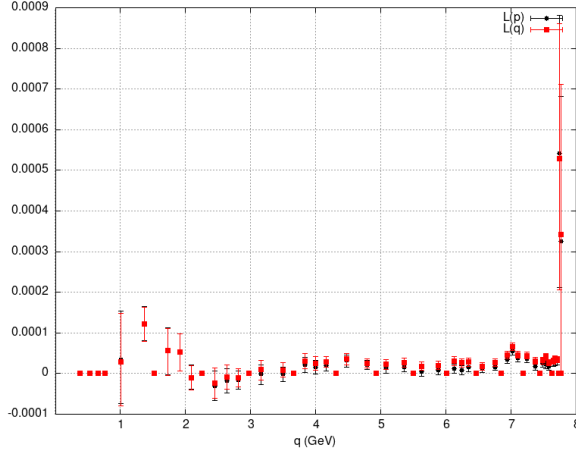
Figure 5.3: Infrared behaviour of the Kugo-Ojima function.

¹In [43] an explicit derivation for this is given, but for the non-expanded system.

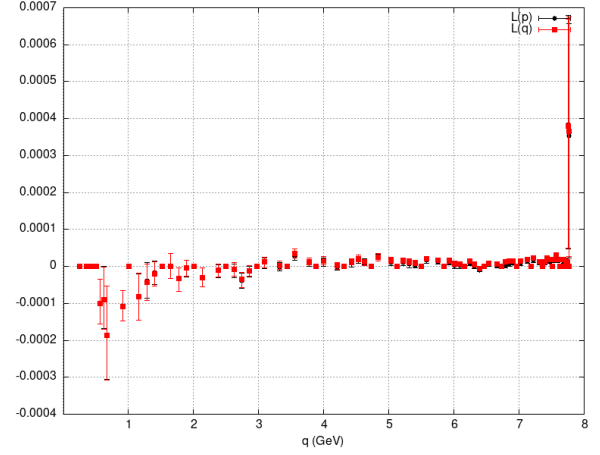
The volume effects appear to be small, as the data for all lattices used seem to agree within the associated uncertainties. However, it is noticeable that the fluctuations in the infrared are greater than in the ultraviolet regime, which is expected, since on the lattice, there are fewer momenta points in the infrared that contribute to the Z_4 averaging mentioned in Section 4.4.3. Additionally, Gribov copies might also contribute to this effect. A conclusion regarding the value of $u(0)$ cannot be drawn yet before renormalizing the function, which we will consider in section 5.6.

5.2 Longitudinal Test

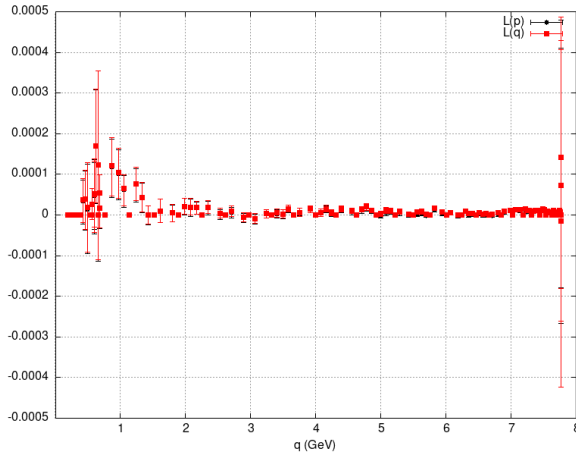
We have performed the longitudinal test mentioned in 4.4.2 for all lattices with both types of momenta, the naive momenta and the improved momenta. In Figure 5.4 we show the results of the longitudinal tests for each lattice:



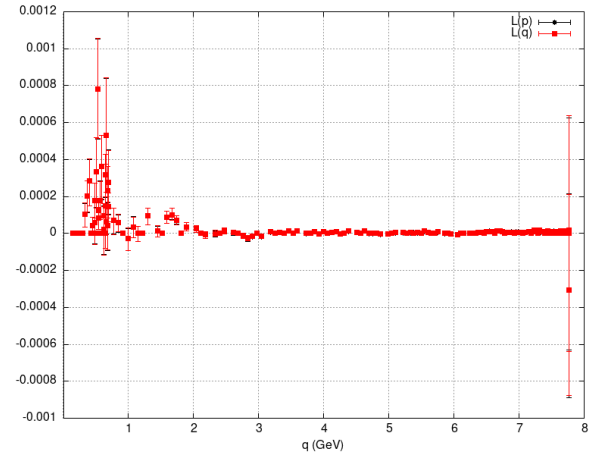
(a) 32^4 Lattice - computed with 300 configurations over 1 source.



(b) 48^4 Lattice - computed with 200 configurations over 2 sources.



(c) 64^4 Lattice - computed with 200 configurations over 2 sources.



(d) 80^4 Lattice - computed with 200 configurations over 1 source.

Figure 5.4: Longitudinal component $L(q)$ of the lattice Kugo-Ojima function.

As we can see, the longitudinal part is negligible ($u(p^2)/L(p) \approx 0.001/0.5 = 0.2\%$) in comparison with the Kugo-Ojima function. At an uncertainty level of 2σ , it is mostly compatible with zero, which is expected. In the infrared, the fluctuations are significantly

greater than in the ultraviolet. These fluctuations are also present in the Kugo-Ojima function itself, as mentioned in the previous section which indicates that the cause of these fluctuations is most likely correlated. For both types of momenta, the longitudinal components are coincident for both the infrared and the ultraviolet region. In the infrared this overlap is expected since both momenta types coincide in the infrared. In the ultraviolet region, both components converge to zero². It should be mentioned however, that only the positive momenta were used in calculating the longitudinal components, since unlike the Kugo-Ojima function, the longitudinal component is not invariant under the action of the H4 group mentioned in section 4.4.3. These findings prove the transversality of the Kugo-Ojima function in the Landau gauge on the lattice.

²Except for the last data point in each graph. This data point corresponds to the momentum $p_\mu = (N(\mu), N(\mu), N(\mu), N(\mu))$. According to (4.5), this momenta is the only of its kind when taking the Z4 average as explained in section 4.4.3, which explains the large uncertainty associated.

5.3 Inclusion of Negative Momenta Points

Initially, the first version of the computation of the Kugo-Ojima function did not include the averages over the negative momenta points and presented a non-zero imaginary part, which is expected from (4.32). The inclusion of negative momenta points in the Z4 averaging process eliminates this imaginary part and improves the statistical accuracy of the data:

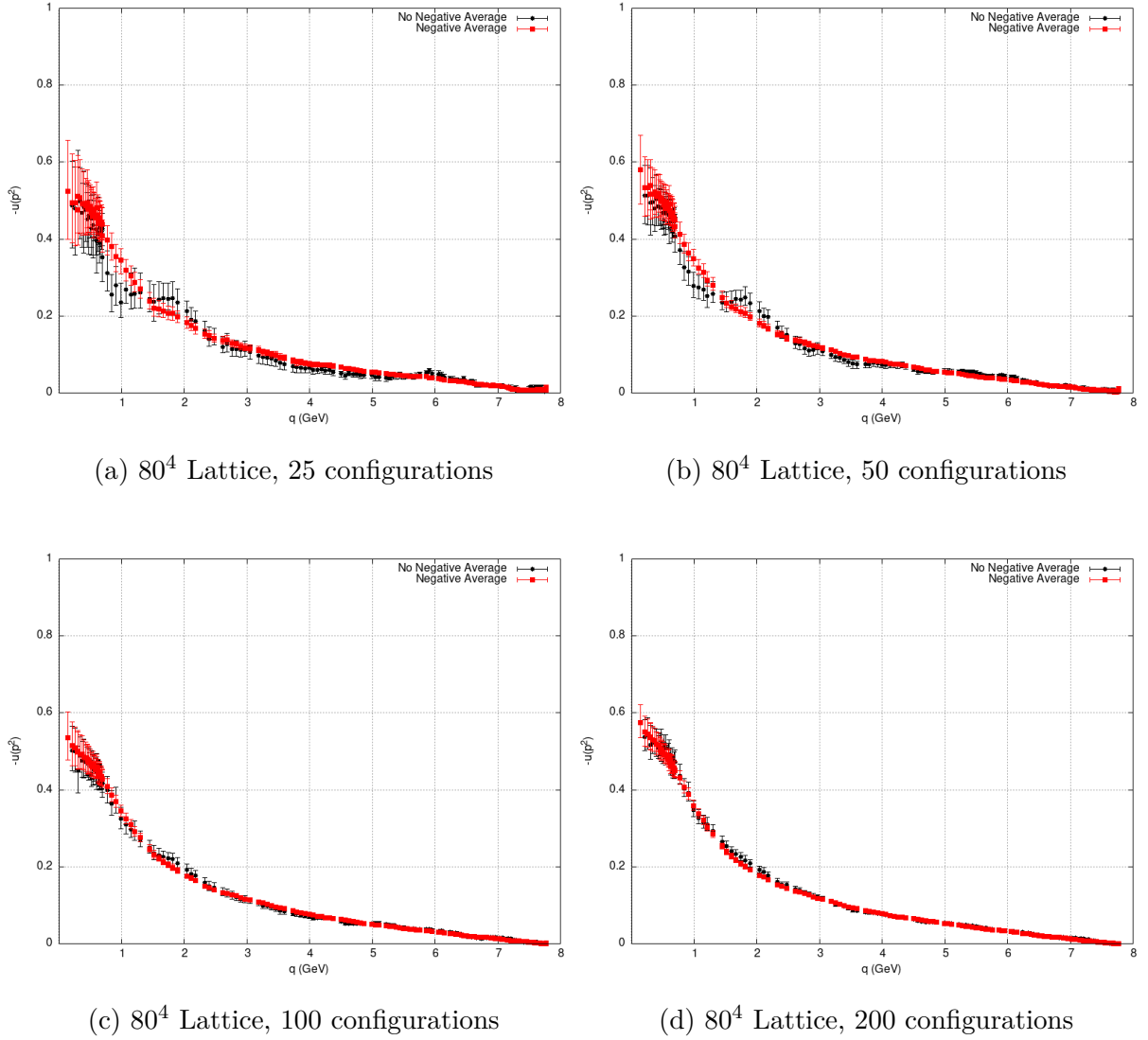


Figure 5.5: Effect of including negative momenta in Z4 averaging process for the 80^4 lattice. All plots have been computed over a single source.

The difference between the two calculations decreases with the number of configurations used for the calculation, but it is noticeable the effects of including the negative momenta

when inspecting the first two plots. The inclusion of negative momenta in our averaging process improves the statistical accuracy of the results, which is to be expected; if one considers only positive components for the momenta point $p_\mu = (p_x, p_y, p_z, p_t)$, there are only $4! \cdot 3! \cdot 2! \cdot 1! = 24$ possible permutations, whereas including the negative components increases this number up to $(2)^4 \cdot 4! \cdot 3! \cdot 2! \cdot 1! = 384$ momenta points included in the averaging process.

5.4 Sources vs Configurations

Ideally, one would compute the Kugo-Ojima function for all possible sources and take the average, which would yield the full *all-to-all* propagator. However, such task is from a computational point of view, very expensive. So, to see what kind of statistical effects additional sources have, we performed the following comparison to the 32^4 and 64^4 lattices:

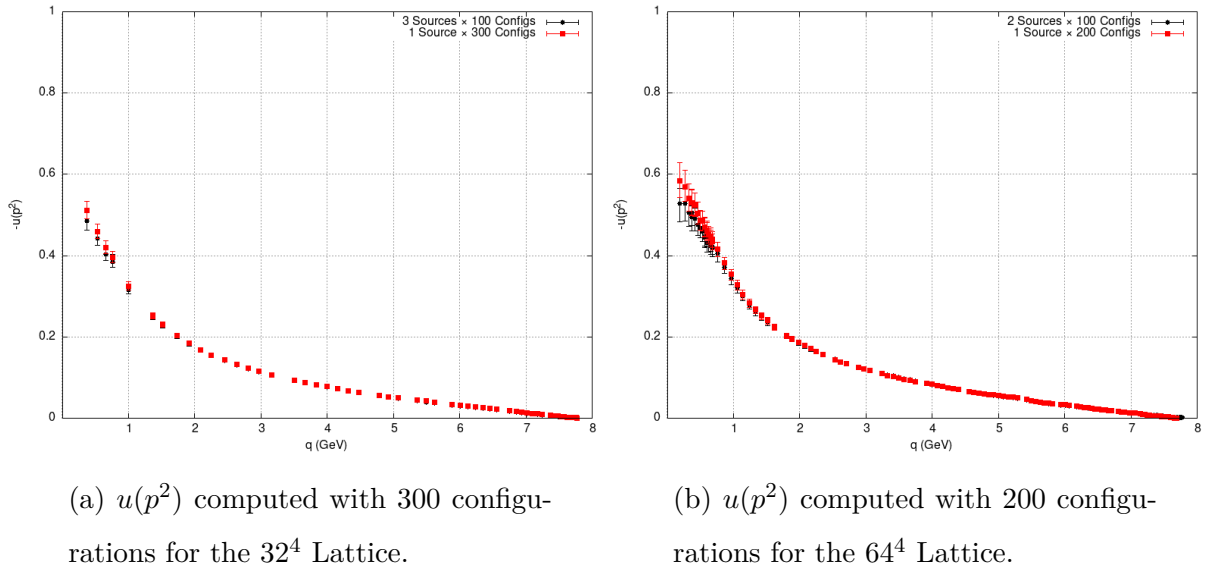
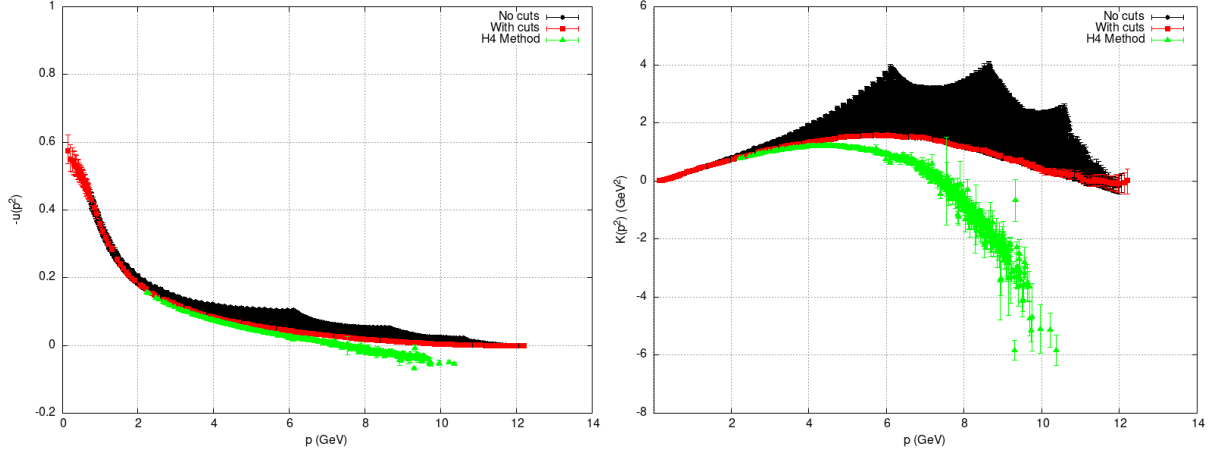


Figure 5.6: Difference between using sources vs configurations.

It is noticeable that the central values are shifted in the right panel, but the points are within one standard deviation. So, since in both cases the uncertainty intervals are similar, we can conclude that considering additional sources yield the same improvement in statistics as including more configurations in the computation. We chose to prioritize the amount of configurations over sources in our calculations, as this is more convenient from the point of view of Monte Carlos sampling.

5.5 H4 method

Following the discussion of section 4.4.3 we compare how the cuts we have been performing so far compare against the H4 method. The comparison is performed for the both the Kugo-Ojima function and its *dressing function* ($K(p^2) = -p^2 u(p^2)$). We consider the data for the largest volume, 80^4 .



(a) The Kugo-Ojima function $u(p^2)$.

(b) Kugo-Ojima's Dressing function $K(p^2)$.

Figure 5.7: Comparing the H4 method with the cuts discussed in 4.4.3 for the Kugo-Ojima function $u(p^2)$ and its dressing function $K(p^2)$. Both plots have been computed with 200 configurations over 1 source.

As we can see, for the infrared ($q \leq 3$ GeV) the H4 method seems to agree with the canonical cuts method, but it seems to overestimate the correction of lattice artifacts outside the infrared region. Unfortunately, the method depends on finding lattice points that have the same $p^{[2]} = p^2$, which in the infrared region are fewer.

5.6 Renormalization of the Kugo-Ojima function

As mentioned in section 5.1, we should renormalize the bare lattice data before drawing any conclusion. To renormalize our lattice bare data we will make use of the Dyson-Schwinger equations results for $u(p^2, \mu^2)$ in [2, 53] and renormalize by setting³

$$Z_u(\mu^2)(1 + u_0(p^2)) = 1 + u(p^2, \mu^2) \quad (5.1)$$

taking the renormalization point to be $\mu = 4.3$ GeV. We perform the renormalization procedure for the two largest lattices 64^4 and 80^4 . Below we present the result of the described renormalization procedure:

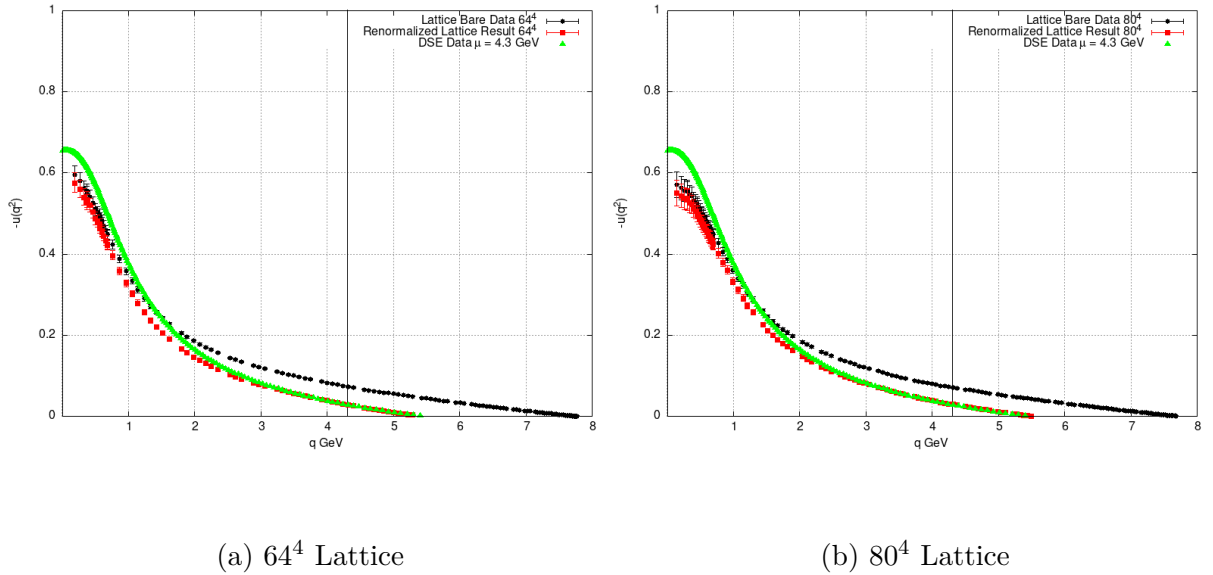


Figure 5.8: The renormalized lattice Kugo-Ojima function compared with the results of [2]. The vertical black bar denotes the $q = 4.3$ GeV line.

It is insightful to repeat the previous plots in a logarithmic scale:

³The results for $u(p^2, \mu^2)$ in [2] were renormalized using the MOM-scheme discussed in section 2.3.2.

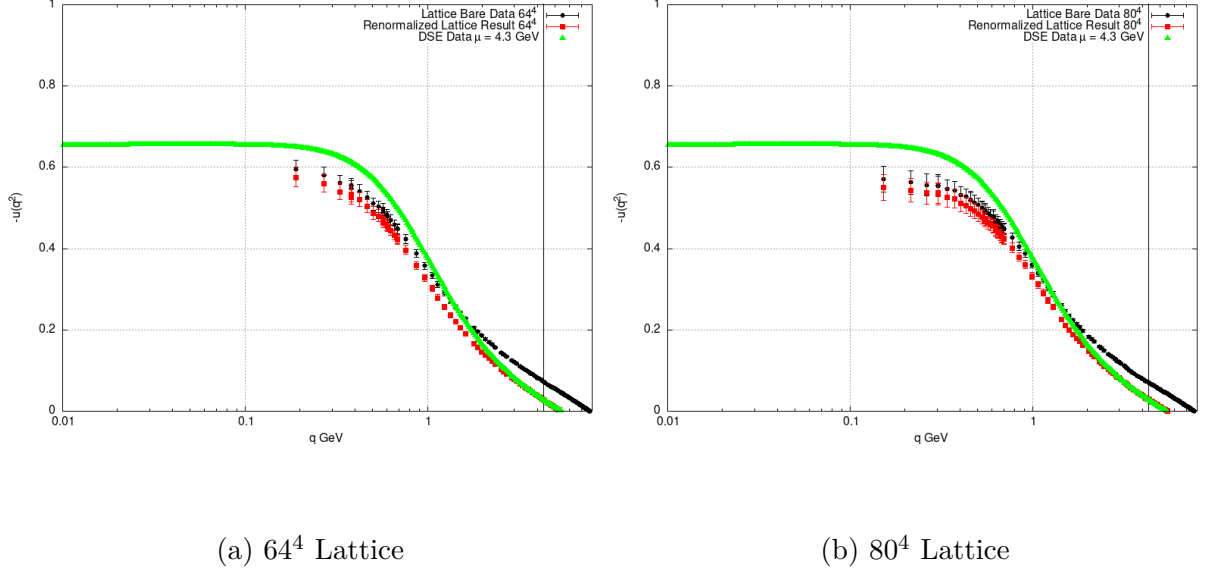


Figure 5.9: Previous figure but in logarithmic scale.

Our results follow the same trend with the lattice data of [39]. Our lattice results are also in qualitative agreement with the DSE result, but with a slight deviation in the infrared region. The reason for this deviation might range from approximations used in both approaches to lattice artifacts.

The previous plots show that extrapolating to the origin would result in $u(0) \neq -1$, which points to the non-realization of the Kugo-Ojima confinement scenario. Inspecting the graphs shows that the extrapolation would result roughly in an upper bound of $u(0, \mu = 4.3 \text{ GeV}) < -0.7$, which is closer to the estimate given by the author of [11] of $u(0) = -\frac{2}{3}$. Furthermore, consider the following identity that relates $u(p^2)$ with the ghost dressing function [8]:

$$J(p^2) = \frac{1}{1 + u(p^2) + p^2 v(p^2)} \quad G^{ab}(p^2) = -\frac{\delta^{ab} J(p^2)}{p^2} \quad (5.2)$$

where $v(p^2)$ is an arbitrary function as stated in [8]. At $p^2 = 0$,

$$J(0) = \frac{1}{1 + u(0)} \quad (5.3)$$

This relation links a diverging ghost dressing function with the realization of the Kugo-Ojima confinement scenario. This would also have to occur for the renormalized ghost dressing function as well which implies that for any renormalization point $u(0, \mu^2) = -1$, making the function RG-independent at the origin. The authors of [54, 2] studied the renormalization dependence of $u(0, \mu^2)$ and verified that there is a renormalization

dependence, making it RG-dependent. Furthermore, there are numerical results that point to a finite ghost dressing function at the origin [55, 56], which further strengthens that the Kugo-Ojima confinement scenario is not likely satisfied. All this evidence for the non-realization of the scenario could point to the non-validity of the assumption of BRST-symmetry at the non-perturbative level or at least in lattice QCD. In section 3.2, it is assumed that Q_B remains unbroken, and it is only under that assumption that the Kugo-Ojima confinement scenario holds. This assumption is not trivial, it is not known if BRST symmetry holds at the non-perturbative regime of gauge theories and in fact, numerical evidence for BRST-symmetry breaking on the lattice have been found [57, 58]. This invalidates the definition given in section 3.2 for the physical subspace $\mathcal{V}_{\text{phys}}$, invalidating the hypothesis from the beginning. We end by noting that the interest in the computation of the Kugo-Ojima function spans beyond just obtaining the value of $u(0)$. The function as a whole is of interest for other studies such as the already mentioned DSE equations [54, 2] or the Gribov-Zwazinger horizon condition [9, 10, 11].

6 Conclusion

Throughout this work, we have discussed the Kugo-Ojima confinement scenario and the important role that the function $u(p^2)$ has in it. A relatively efficient method is presented for its lattice computation at all the possible momenta values.

We start by presenting lattice bare data of the Kugo-Ojima function in the Landau gauge, studying the lattice volume dependence, the longitudinal part, which is compatible with zero, as expected. A statistical analysis of the computation, followed by the renormalized result was also presented.

Our results are in good agreement with the lattice data of [39] and also supports the estimated provided in [11]. The results present evidence for the non-realization of the Kugo-Ojima confinement scenario, which agrees with literature studies performed using different formalisms. These studies include the RG-dependence of $u(0, \mu^2)$ [2, 54], the non-enhanced ghost dressing function [55, 56] and BRST-Symmetry breaking [57, 58]. This last one could be the core reason for the non-realization of the confinement scenario. A possible reason for the non-realization of the confinement scenario is that the assumption that the BRST-charge remains unbroken is not valid. Indeed, this is not a trivial assumption, since the BRST-symmetry lacks proof of its validity at the non-perturbative level. A broken BRST-charge implies that we cannot use it to define the physical subspace as we did in Section 3.2.1.

In the future, efforts will be made towards improving the statistics of the data presented and further optimization improvements can be considered. It would also be interesting to see how the Kugo-Ojima function would look on larger lattices or different gauges, although the computational resources required can be significantly high to consider other gauges.

Bibliography

- [1] C. Gattringer and C. Lang, *Quantum chromodynamics on the lattice: an introductory presentation*, vol. 788. Springer Science & Business Media, 2009.
- [2] A. C. Aguilar, D. Binosi, and J. Papavassiliou, “Indirect determination of the Kugo-Ojima function from lattice data,” *Journal of High Energy Physics*, vol. 2009, no. 11, p. 066, 2009.
- [3] S. N. Gupta, “Theory of longitudinal photons in quantum electrodynamics,” *Proceedings of the Physical Society. Section A*, vol. 63, no. 7, p. 681, 1950.
- [4] K. Bleuler, “Eine neue Methode zur Behandlung der longitudinalen und skalaren Photonen,” *Helvetica Physica Acta*, vol. 23, no. 5, pp. 567–586, 1950.
- [5] T. Kugo and I. Ojima, “Local covariant operator formalism of non-Abelian gauge theories and quark confinement problem,” *Progress of Theoretical Physics Supplement*, vol. 66, pp. 1–130, 1979.
- [6] C. Becchi, A. Rouet, and R. Stora, “Renormalization of gauge theories,” *Annals of Physics*, vol. 98, no. 2, pp. 287–321, 1976.
- [7] I. V. Tyutin, “Gauge invariance in field theory and statistical physics in operator formalism,” *arXiv preprint arXiv:0812.0580*, 2008.
- [8] T. Kugo, “The Universal renormalization factors $Z(1) / Z(3)$ and color confinement condition in non-Abelian gauge theory,” *arXiv preprint hep-th/9511033*, pp. 107–119, 7 1995.
- [9] D. Zwanziger, “Local and renormalizable action from the Gribov horizon,” *Nuclear Physics B*, vol. 323, no. 3, pp. 513–544, 1989.

- [10] D. Dudal, S. P. Sorella, N. Vandersickel, and H. Verschelde, “Gribov no-pole condition, Zwanziger horizon function, Kugo-Ojima confinement criterion, boundary conditions, BRST breaking and all that,” *Phys. Rev. D*, vol. 79, p. 121701, 2009.
- [11] K.-I. Kondo, “Kugo–Ojima color confinement criterion and Gribov–Zwanziger horizon condition,” *Physics Letters B*, vol. 678, no. 3, pp. 322–330, 2009.
- [12] M. N. Ferreira and J. Papavassiliou, “Gauge sector dynamics in QCD,” *Particles*, vol. 6, no. 1, pp. 312–363, 2023.
- [13] R. P. Feynman, A. R. Hibbs, and D. F. Styer, *Quantum mechanics and path integrals*. Courier Corporation, 2010.
- [14] W. Greiner and J. Reinhardt, *Field quantization*. Springer Science & Business Media, 1996.
- [15] A. L. Fetter and J. D. Walecka, *Quantum theory of many-particle systems*. Courier Corporation, 2012.
- [16] K. Osterwalder and R. Schrader, “Axioms for Euclidean Green’s functions II,” *Communications in Mathematical Physics*, vol. 42, no. 3, pp. 281–305, 1975.
- [17] L. D. Faddeev and V. N. Popov, “Feynman diagrams for the Yang-Mills field,” *Physics Letters B*, vol. 25, no. 1, pp. 29–30, 1967.
- [18] L. H. Ryder, *Quantum field theory*. Cambridge university press, 1996.
- [19] M. E. Peskin, *An introduction to quantum field theory*. CRC press, 2018.
- [20] V. N. Gribov, “Quantization of non-Abelian gauge theories,” *Nuclear Physics B*, vol. 139, no. 1-2, pp. 1–19, 1978.
- [21] I. M. Singer, “Some remarks on the Gribov ambiguity,” *Communications in Mathematical Physics*, vol. 60, pp. 7–12, 1978.
- [22] T. Killingback, “The Gribov ambiguity in gauge theories on the four-torus,” *Physics Letters B*, vol. 138, no. 1-3, pp. 87–90, 1984.
- [23] D. Zwanziger, “Renormalizability of the critical limit of lattice gauge theory by BRS invariance,” *Nuclear Physics B*, vol. 399, no. 2-3, pp. 477–513, 1993.

- [24] P. van Baal, “More (thoughts on) Gribov copies,” *Nuclear Physics B*, vol. 369, no. 1-2, pp. 259–275, 1992.
- [25] G. Dell’Antonio and D. Zwanziger, “Every gauge orbit passes inside the Gribov horizon,” *Communications in mathematical physics*, vol. 138, no. 2, pp. 291–299, 1991.
- [26] R. Alkofer and L. Von Smekal, “The infrared behaviour of QCD Green’s functions: confinement, dynamical symmetry breaking, and hadrons as relativistic bound states,” *Physics Reports*, vol. 353, no. 5-6, pp. 281–465, 2001.
- [27] W. Celmaster and R. J. Gonsalves, “Renormalization-prescription dependence of the quantum-chromodynamic coupling constant,” *Phys. Rev. D*, vol. 20, pp. 1420–1434, Sep 1979.
- [28] N. Nakanishi and I. Ojima, *Covariant operator formalism of gauge theories and quantum gravity*. World Scientific, 1990.
- [29] N. Nakanishi, “Covariant quantization of the electromagnetic field in the Landau gauge,” *Progress of Theoretical Physics*, vol. 35, no. 6, pp. 1111–1116, 1966.
- [30] I. Ojima, “Observables and quark confinement in the covariant canonical formalism of Yang-Mills theory,” *Nuclear Physics B*, vol. 143, no. 2, pp. 340–352, 1978.
- [31] I. J. R. Aitchison and A. J. Hey, *Gauge theories in particle physics, Volume II: QCD and the Electroweak Theory*. CRC Press, 2003.
- [32] K. G. Wilson, “Confinement of quarks,” *Phys. Rev. D*, vol. 10, pp. 2445–2459, Oct 1974.
- [33] O. Oliveira and P. Silva, “Gribov copies and gauge fixing in lattice gauge theories,” *Nuclear Physics B-Proceedings Supplements*, vol. 106, pp. 1088–1090, 2002.
- [34] O. Oliveira and P. Silva, “A global optimization method for Landau gauge fixing in lattice QCD,” *Computer physics communications*, vol. 158, no. 2, pp. 73–88, 2004.
- [35] P. J. Silva and O. Oliveira, “Gauge fixing methods and Gribov copies effects in lattice QCD,” *PoS*, vol. LATTICE2007, p. 333, 2007.

- [36] C. Davies, G. Batrouni, G. Katz, A. S. Kronfeld, G. Lepage, K. Wilson, P. Rossi, and B. Svetitsky, “Fourier acceleration in lattice gauge theories. I. Landau gauge fixing,” *Physical Review D*, vol. 37, no. 6, p. 1581, 1988.
- [37] P. Silva and O. Oliveira, “Gribov copies, lattice QCD and the gluon propagator,” *Nuclear Physics B*, vol. 690, no. 1-2, pp. 177–198, 2004.
- [38] A. Cucchieri and T. Mendes, “1) The influence of Gribov copies on gluon and ghost propagators in Landau gauge and 2) A new implementation of the fourier acceleration method,” *Nuclear Physics B-Proceedings Supplements*, vol. 63, no. 1-3, pp. 841–843, 1998.
- [39] A. Sternbeck, “The infrared behavior of lattice QCD Green’s functions,” *arXiv preprint hep-lat/0609016*, 2006.
- [40] A. Cucchieri, D. Dudal, T. Mendes, O. Oliveira, M. Roelfs, and P. J. Silva, “Faddeev-Popov matrix in linear covariant gauge: First results,” *Physical Review D*, vol. 98, no. 9, p. 091504, 2018.
- [41] A. Cucchieri, D. Dudal, T. Mendes, O. Oliveira, M. Roelfs, and P. J. Silva, “Lattice Computation of the Ghost Propagator in Linear Covariant Gauges,” *PoS*, vol. LATTICE2018, p. 252, 2018.
- [42] D. Zwanziger, “Fundamental modular region, Boltzmann factor and area law in lattice theory,” *Nuclear Physics B*, vol. 412, no. 3, pp. 657–730, 1994.
- [43] P. Boucaud, J. Leroy, A. Le Yaouanc, A. Lokhov, J. Micheli, O. Pene, J. Rodriguez-Quintero, and C. Roiesnel, “Large momentum behavior of the ghost propagator in SU (3) lattice gauge theory,” *Physical Review D*, vol. 72, no. 11, p. 114503, 2005.
- [44] R. Barrett, M. Berry, T. F. Chan, J. Demmel, J. Donato, J. Dongarra, V. Eijkhout, R. Pozo, C. Romine, and H. Van der Vorst, *Templates for the solution of linear systems: building blocks for iterative methods*. SIAM, 1994.
- [45] H. Suman and K. Schilling, “First lattice study of ghost propagators in SU (2) and SU (3) gauge theories,” *Physics Letters B*, vol. 373, no. 4, pp. 314–318, 1996.

- [46] F. T. Winter, M. A. Clark, R. G. Edwards, and B. Joó, “A framework for lattice QCD calculations on GPUs,” in *2014 IEEE 28th International Parallel and Distributed Processing Symposium*, pp. 1073–1082, IEEE, 2014.
- [47] R. G. Edwards and B. Joo, “The Chroma software system for lattice QCD,” *arXiv preprint hep-lat/0409003*, 2004.
- [48] M. Pippig, “PFFT: An extension of FFTW to massively parallel architectures,” *SIAM Journal on Scientific Computing*, vol. 35, no. 3, pp. C213–C236, 2013.
- [49] R. Gupta, “Introduction to lattice QCD,” *arXiv preprint hep-lat/9807028*, 1998.
- [50] F. De Soto and C. Roiesnel, “On the reduction of hypercubic lattice artifacts,” *Journal of High Energy Physics*, vol. 2007, no. 09, p. 007, 2007.
- [51] D. B. Leinweber, J. I. Skullerud, A. G. Williams, and C. Parrinello, “Asymptotic scaling and infrared behavior of the gluon propagator,” *Physical Review D*, vol. 60, no. 9, p. 094507, 1999.
- [52] G. S. Bali and K. Schilling, “Running coupling and the Λ parameter from SU (3) lattice simulations,” *Physical Review D*, vol. 47, no. 2, p. 661, 1993.
- [53] M. N. Ferreira. personal communication.
- [54] D. Binosi, “On the dynamics of the Kugo-Ojima function,” *PoS*, vol. QCD-TNT09, p. 004, 2009.
- [55] P. Boucaud, J. Leroy, A. Le Yaouanc, J. Micheli, O. Pene, and J. Rodríguez-Quintero, “On the IR behaviour of the Landau-gauge ghost propagator,” *Journal of High Energy Physics*, vol. 2008, no. 06, p. 099, 2008.
- [56] A. Cucchieri and T. Mendes, “What’s up with IR gluon and ghost propagators in Landau gauge? A puzzling answer from huge lattices,” *arXiv preprint arXiv:0710.0412*, 2007.
- [57] A. Cucchieri, D. Dudal, T. Mendes, and N. Vandersickel, “Evidence of BRST-Symmetry Breaking in Lattice Minimal Landau Gauge,” *arXiv preprint arXiv:1410.8410*, 2014.

- [58] S. W. Li, P. Lowdon, O. Oliveira, and P. J. Silva, “Non-perturbative BRST symmetry and the spectral structure of the ghost propagator,” *Physics Letters B*, vol. 823, p. 136753, 2021.

Appendix A

Parallel Transporter

In this appendix, we motivate the definition of the link variable provided in (4.8). Having our space discretized into a lattice, the derivative should be replaced by one of the following finite difference formula:

$$\begin{aligned}\partial_\mu f(x) &= \frac{f(x + a\hat{\mu}) - f(x)}{a} + \mathcal{O}(a^2), \\ \partial_\mu f(x) &= \frac{f(x + a\hat{\mu}) - f(x - a\hat{\mu})}{2a} + \mathcal{O}(a^3)\end{aligned}\tag{A.1}$$

where $\hat{\mu}$ is the unit vector in the μ direction. The first option should be closer to its continuum counter-part than the second, but at the expense of a less rigorous approximation. In this work, the lattice spacing a should be small enough to use the first option. Consider an arbitrary field $\phi(x)$ that transforms under some representation of a given Lie Group G :

$$\phi(x) \longrightarrow \phi'(x) = G(x)\phi(x).\tag{A.2}$$

The corresponding kinetic term $(\partial_\mu\phi(x))^\dagger(\partial^\mu\phi(x))$ will have products like $\phi(x+a\hat{\mu})^\dagger\phi(x)$ which, in general, explicitly violates gauge invariance. Gauge invariance is restored by introducing the parallel transporter $\Lambda(x, y)$ [19]:

$$\Lambda(x, y) = P \exp\left(ig \int_{\mathcal{C}_{xy}} A^\mu ds_\mu\right)\tag{A.3}$$

where the P stands for *path-ordered* integral¹. The g is the coupling constant associated with the gauge fields. The respective transformation law is given by [19]:

$$\Lambda(x, y) \longrightarrow G(x)\Lambda(x, y)G^{-1}(y) = G(x)\Lambda(x, y)G^\dagger(y).\tag{A.4}$$

¹Let $s \in [0, 1]$ be a parametrization of the path \mathcal{C}_{xy} . The path-ordering prescription will order the $A^\mu(x(s))$ in the exponential so that higher values of s are on the left. It is similar to *time-ordering* integral in the canonical treatment of field theories.

Now, terms like $\phi(x)^\dagger \Lambda(x, y) \phi(y)$ are gauge invariant. For small lattice spacing:

$$\Lambda(x, x + a\hat{\mu}) = p \exp \left(ig \int_x^{x+a\hat{\mu}} A_\mu^a(x) t^a dx^\mu \right) \approx \exp \left(ig \frac{a}{2} A_\mu^a \left(x + \frac{a}{2} \hat{\mu} \right) t^a \right) \quad (\text{A.5})$$

which is the expression in (4.8).

Appendix B

Gauge Fixing Functional

In this appendix, we prove that optimizing the functional:

$$F_U[G] = A \sum_{x,\mu} \text{Re} \left[\text{Tr} \left\{ G(x) U_\mu(x) G^\dagger(x + a\hat{\mu}) \right\} \right] \quad (\text{B.1})$$

corresponds to fixing the Landau gauge for the input configuration. Near the maximum of $F_U[G]$, we can expand the functional as:

$$F_U[\mathbf{1} + i\alpha^a(x)t^a] \approx F_U[\mathbf{1}] + \frac{A}{4} \sum_{x,\mu} i\alpha^a(x) \text{Tr} \left\{ t^a \left[(U_\mu(x) - U_\mu(x - \hat{\mu}) - (U_\mu^\dagger(x) - U_\mu^\dagger(x - \hat{\mu}))) \right] \right\}. \quad (\text{B.2})$$

A stationary point of the functional, such as a maximum, will obey:

$$\frac{\partial F}{\partial \alpha^a(x)} = \frac{iA}{4} \sum_{\mu} \text{Tr} \left\{ t^a \left[(U_\mu(x) - U_\mu(x - \hat{\mu}) - (U_\mu^\dagger(x) - U_\mu^\dagger(x - \hat{\mu}))) \right] \right\} = 0. \quad (\text{B.3})$$

Using the definition of link (4.8):

$$\sum_{\mu} \text{Tr} \left\{ t^a \left[A_\mu \left(x + \frac{a}{2} \hat{\mu} \right) - A_\mu \left(x - \frac{a}{2} \hat{\mu} \right) \right] \right\} + \mathcal{O}(a^2) = 0. \quad (\text{B.4})$$

Performing a Taylor expansion of the gluon fields yields:

$$\sum_{\mu} \partial_\mu A_\mu^a(x) + \mathcal{O}(a^2) = 0 \quad (\text{B.5})$$

which concludes the proof. Furthermore, note that maximizing the functional $F_U[G]$ also means setting its second derivative to be negative. Looking at equation (B.5), it is possible to conclude that the second variation of the functional $F_U[G]$ is the symmetry Faddeev-Popov matrix (i.e $-M[A; x, y]^{ab}$ in (2.22)). So, maximizing this functional means restricting the space of configurations to Ω .

Appendix C

Point Source Generation

In this appendix we prove the relation provided in equation (4.42):

$$\sum_c f_{abc} A_\mu^c(x) = -\frac{1}{2} \text{Tr} \left[\left\{ \left(U_{-\mu}^\dagger(x) + U_\mu(x) \right) - \left(U_{-\mu}^\dagger(x) + U_\mu(x) \right)^\dagger \right\} [t^a, t^b] \right]. \quad (\text{C.1})$$

First, we multiply the gauge field $A_\mu \left(x + \frac{\hat{\mu}}{2} \right)$ by the Lie algebra commutator:

$$A_\mu \left(x + \frac{\hat{\mu}}{2} \right) [t^a, t^b] = A_\mu \left(x + \frac{\hat{\mu}}{2} \right) i \sum_c f_{abc} t^c. \quad (\text{C.2})$$

Using expression (4.9) on the left-hand side yields:

$$\begin{aligned} \left(\frac{1}{2ig_0} \left(U_\mu(x) - U_\mu^\dagger(x) \right) - \frac{1}{6ig_0} \text{Tr} \left\{ U_\mu(x) - U_\mu^\dagger(x) \right\} \right) [t^a, t^b] &= \\ &= \sum_{c,d} i f_{abc} A_\mu^d \left(x + \frac{\hat{\mu}}{2} \right) t^d t^c. \end{aligned} \quad (\text{C.3})$$

Taking the trace on both sides and using (2.3):

$$\frac{1}{ig_0} \text{Tr} \left\{ \left(U_\mu(x) - U_\mu^\dagger(x) \right) [t^a, t^b] \right\} = \sum_c i f_{abc} A_\mu^c \left(x + \frac{\hat{\mu}}{2} \right). \quad (\text{C.4})$$

The second term on the left hand side in (C.3) is traceless because of the SU(3) Lie algebra (2.3). Performing a Taylor expansion on the right-hand side up to $\mathcal{O}(a^2)$ and multiplying by $-i$ allows us to write:

$$-\frac{1}{g_0} \text{Tr} \left\{ \left(U_\mu(x) - U_\mu^\dagger(x) \right) [t^a, t^b] \right\} = \sum_c f_{abc} \left(A_\mu^c(x) + \frac{a}{2} \partial_\mu A_\mu^c(x) + \mathcal{O}(a^2) \right). \quad (\text{C.5})$$

Using the same formula for $x - \frac{\hat{\mu}}{2}$, we get:

$$\begin{aligned} -\frac{1}{g_0} \text{Tr} \left\{ \left(U_\mu(x - a\hat{\mu}) - U_\mu^\dagger(x - a\hat{\mu}) \right) [t^a, t^b] \right\} &= \\ &= \sum_c f_{abc} \left(A_\mu^c(x) - \frac{a}{2} \partial_\mu A_\mu^c(x) + \mathcal{O}(a^2) \right) \end{aligned} \quad (\text{C.6})$$

Using (4.10) and summing the last 2 equations, yields:

$$\sum_c f_{abc} A_\mu^c(x) = -\frac{1}{2g_0} \text{Tr} \left[\left\{ (U_{-\mu}^\dagger(x) + U_\mu(x)) - (U_{-\mu}^\dagger(x) + U_\mu(x))^\dagger \right\} [t^a, t^b] \right] \quad (\text{C.7})$$

which concludes the demonstration. To end, we note that we will set $\beta = 6.0$ which implies for $N_c = 3$ that the bare coupling constant is set to one $g_0 = 1$.